Ross scheme, Newton-Raphson iterative methods and time-stepping strategies for solving the mixed-form of Richards' equation

Hassane[1,2] Maina F., Ackerer[1,*] P.

[1]Laboratoire d'Hydrologie et de Géochimie de Strasbourg,
Univ. Strasbourg/EOST - CNRS
1 rue Blessig, 67084 Strasbourg,
France

[2]CEA-Laboratoire de Modélisation des Transferts dans l'Environnement,
Bât. 225, F-13108 Saint Paul lez Durance cedex,
France

*Corresponding author: ackerer@unistra.fr

ABSTRACT

The solution of the mathematical model for flow in variably saturated porous media described by Richards equation (RE) is subject to heavy numerical difficulties due to its highly non-linear properties and remains very challenging. Two different algorithms are used in this work to solve the mixed-form of RE: the traditional iterative algorithm and a time-adaptive algorithm consisting of changing the time step magnitude within the iteration procedure while the non-linear parameters are computed with the state variable at the previous time. The Ross method is an example of this type of scheme, and we show that it is equivalent to the Newton-Raphson method with a time-adaptive algorithm.

Both algorithms are coupled to different time stepping strategies: the standard heuristic approach based on the number of iterations and two strategies based on the time truncation error or on the change of water saturation. Three different test cases are used to evaluate the efficiency of these algorithms.

The numerical results highlight the necessity of implementing an estimate of the time truncation errors.

1. Introduction

Water movement in soils is one of the key processes in the water cycle since it contributes to the renewal of groundwater resources through recharge, to vegetation growth through transpiration, to soil fertility through salinization/alteration and to atmospheric humidity through evaporation and transpiration. Water movement is usually modeled using the Richards equation (Richards, 1931), which is now commonly adopted for many studies in soil science and/or hydrology, including the use of physically based hydrological models applied to large-scale catchments and for long time simulations (e.g., for climate change studies). However, this equation is highly nonlinear and despite numerous efforts over the last 40 years, its numerical solution requires much computational time.

Assuming a rigid solid matrix, the Richards equation (RE) is given by,

$$\begin{cases} \dfrac{\partial \theta}{\partial t} + S_w s_0 \dfrac{\partial \psi}{\partial t} + \nabla \cdot \mathbf{q} = f \\ \mathbf{q} = -k_r(\psi)\mathbf{K}\left[\nabla \psi + \nabla z\right] \end{cases} \tag{1}$$

where θ is the volumetric water content [L^3/L^3], S_w is the water saturation [-], s_0 accounts for fluid compressibility [L^{-1}], ψ is the pressure head [L], $\mathbf{q}$ is the water flux based on the extended Darcy's law [L/T], t is the time [T], z is the vertical coordinate (positive upward) [L], f is the sink/source term [T^{-1}], $\mathbf{K}$ is the saturated hydraulic conductivity tensor [L/T] and $k_r(\psi)$ is the relative hydraulic conductivity [-]. The model includes initial and boundary conditions of the Dirichlet (prescribed pressure head) or Neumann (prescribed flux) type.

Equation (1) is also called the mixed form of RE. Two alternative formulations of the mixed form exist for RE.

The pressure form is defined by:

$$\begin{cases} \left[C(\psi) + S_w s_0\right]\dfrac{\partial \psi}{\partial t} + \nabla \cdot \mathbf{q} = f \\ \mathbf{q} = -k_r(\psi)\mathbf{K}\left[\nabla \psi + \nabla z\right] \end{cases} \tag{2}$$

where $C(\psi) = \dfrac{\partial \theta}{\partial \psi}$ is the specific moisture capacity [L^{-1}], and the soil moisture form that is

restricted to unsaturated conditions is defined by:

$$\begin{cases} \dfrac{\partial \theta}{\partial t} + \nabla \cdot \mathbf{q} = f \\ \mathbf{q} = -\left(\mathbf{D}(\theta)\nabla\theta + k_r(\theta)\mathbf{K}\nabla z \right) \end{cases} \tag{3}$$

where $\mathbf{D}(\theta) = k_r(\theta)\mathbf{K}\dfrac{d\psi}{d\theta}$ is the pore water diffusivity [L^2/T].

Constitutive relations are required to solve RE. For the pressure-water content relationship,

the most common model is the Van Genuchten model (van Genuchten, 1980):

$$S_w(\psi) = \frac{\theta(\psi) - \theta_r}{\theta_s - \theta_r} = \begin{cases} \left(1 + |\alpha\psi|^\eta \right)^{-m} & \psi < 0 \\ 1 & \psi \geq 0 \end{cases} \tag{4}$$

where $m = 1 - 1/\eta$, S_w is the effective saturation, θ_r and θ_s are the residual and saturated

volumetric water content respectively, α and η are experimentally estimated coefficients.

This model is usually associated with Mualem model (Mualem, 1976) for the relative

permeability of the aqueous phase:

$$k_r(S_w) = \begin{cases} S_w^{1/2}\left[1 - \left(1 - S_w^{1/m} \right)^m \right]^2 & \psi < 0 \\ 1.0 & \psi \geq 0 \end{cases} \tag{5}$$

A summary of the most popular relations can be found in Belfort et al. (2013).

Due to the strong heterogeneities of the unsaturated zone and nonlinearities in the constitutive

relations (Eq. (4) and (5)), analytical solution of RE does not exist except in special cases

(Celia et al., 1990; van Dam and Feddes, 2000). Therefore, numerical methods such as finite

difference (Feddes et al., 1988; Romano et al., 1998; van Dam and Feddes, 2000), finite

element (Gottardi and Venutelli, 2001), and mixed finite element (Bause and Knabner, 2004; Bergamaschi and Putti, 1999; Fahs et al., 2009; Farthing et al., 2003) are used to solve RE.

Iterative methods based on the Picard (fixed point) or Newton-Raphson approach (Lehmann and Ackerer, 1998; Paniconi and Putti, 1994) are the most popular techniques for solving this highly nonlinear equation. Alternative iterative methods are based on transform formulations (Crevoisier et al., 2009; Ross and Bristow, 1990; Williams et al., 2000; Zha et al., 2013) or the method of lines (Fahs et al., 2009; Matthews et al., 2004; Miller et al., 1998; Tocci et al., 1997).

Adaptive time stepping strategies based on time truncation error control were found to be superior to others approaches (Hirthe and Graf, 2012; Kavetski et al., 2001; Tocci et al., 1997). The Method of Lines using the DASPK integrator was applied to the Richards' equation by Matthews et al. (2004), Miller et al. (1998), Tocci et al. (1997) among others. The Method of Lines consists of discretization of the spatial part of the PDE only, leading to a system of ordinary differential equations. It has been found to be significantly more efficient than other temporal discretizations (Miller et al., 2006). However, Kavetski and Binning (2002b) reported difficulties in obtaining convergence for the DASPK solver associated with an arithmetic mean of inter-block conductivities for the most difficult problem addressed by Miller et al. (1998). Additionally, very few non-iterative schemes have been developed (Kavetski and Binning, 2004, 2002a; Paniconi et al., 1991).

Despite the many existing numerical methods, solution of the RE is still a challenging research topic with many remaining questions about reduction of the computational time, treatment of nonlinearities, and improvement of the accuracy of these methods for difficult problems such as infiltration in very dry soils (Diersch and Perrochet, 1999; Forsyth et al.,

1995; R. G. Hills, 1989). The need of efficient algorithms for solving this equation has increased during the last decades because it has been recognized that explicit modelling of flow in the unsaturated zone has to be implemented in Land Surface Models (Vergnes et al., 2012). In their recent review of land surface models, Clarke et al. (2015) push for a mechanistic modelling of the flow in soils. They consider that the implementation of the mixed form of the Richards equation is an improvement of the modeling of soil moisture variations. They also underline the need of efficient algorithms for solving the RE to allow the implementation of stochastic approaches and/or automatic parameter estimations.

In this study, we analyzed the performance of different algorithms based on the Newton-Raphson method since the classical Picard scheme has been found less efficient (Lehmann and Ackerer, 1998). Applied to the soil moisture form of the RE equation, we demonstrate that the recently developed Ross method (Ross, 2003; Crevoisier et al., 2009; Zha et al., 2013) is equivalent to Newton-Raphson method (section 2). A detailed presentation of the Newton-Raphson method applied to the mixed form or RE is given in section 3. The standard Newton-Raphson algorithm is based on the computation of the corresponding matrices in an iterative way by updating the parameters until convergence. An alternative algorithm has been suggested more recently where the parameters are kept unchanged within one time step and the time step is adapted to reach convergence. This algorithm has been applied to the pressure-based form of RE by Kavetski and Binning (2002a) and to the soil moisture form by Crevoisier et al. (2009), Ross (2003), Zha et al. (2013). Although this algorithm is called "non iterative" because the parameters are not updated during the calculation, iterations may be necessary to adapt the magnitude of the time step. Therefore, in the following, we will refer to the usual algorithm as "iterative" and to the alternative algorithm as "time-adaptive". To our knowledge, this alternative algorithm has never been applied to the mixed form of RE. Section 4 is dedicated to both algorithms and to the time stepping strategy used for solving

RE. Finally, in section 5, the numerical accuracy and robustness of the algorithms applied to the mixed-form of RE are evaluated using three different test cases.

2. The Ross method and the Newton-Raphson method

The moisture-based formulation is applicable in unsaturated conditions only and is prone to numerical difficulties in the case of heterogeneous soils, explaining the reduced attention directed to this formulation. However, discontinuous water content can be handled by adapted schemes and moisture-based formulation appears to be very accurate for initially dry conditions (Zha et al., 2013, 2015).

Ross (2003) suggested a non-iterative formulation that has been recently extended to different soil conditions (Crevoisier et al., 2009; Varado et al., 2006a) and to two and three dimensions (Zha et al., 2013).

In its initial one-dimensional finite-volume formulation and for a volume (cell) i, the Ross method (Ross, 2003) is based on the following set of equations:

$$\frac{\Delta z}{\Delta t}\left(\theta_i^{n+1} - \theta_i^n\right) = \frac{\Delta z}{\Delta t}\left(\theta_{s,i} - \theta_{r,i}\right)\left(S_i^{n+1} - S_i^n\right) = q_-^\sigma - q_+^\sigma \tag{6}$$

with:

$$\begin{cases} q_+^\sigma = q_+^n + \sigma\left[\left(\frac{\partial q_i^n}{\partial S_i^n}\right)\left(S_i^{n+1} - S_i^n\right) + \left(\frac{\partial q_i^n}{\partial S_{i+1}^n}\right)\left(S_{i+1}^{n+1} - S_{i+1}^n\right)\right] \\ q_-^\sigma = q_-^n + \sigma\left[\left(\frac{\partial q_i^n}{\partial S_i^n}\right)\left(S_i^{n+1} - S_i^n\right) + \left(\frac{\partial q_i^n}{\partial S_{i-1}^n}\right)\left(S_{i-1}^{n+1} - S_{i-1}^n\right)\right] \end{cases} \tag{7}$$

where S_i^{n+1} is the water saturation at cell/node i at time $(n+1)$, q_-^σ (resp. q_+^σ) is the water flux between cell i and $(i-1)$ (resp. $i+1$) at time $t = t^n + \sigma\,\Delta t$, $\sigma \in [0,1]$ and Δz is the size of the cell i. $\theta_{s,i}$ is the saturated water content and $\theta_{r,i}$ is the residual water content. For simplicity, we assume here that all cells are of the same size.

The previous mass balance equation (6) leads to the following equation for cell i:

$$-\left(\frac{\partial q_-^n}{\partial S_{i-1}^n}\right)\left(S_{i-1}^{n+1} - S_{i-1}^n\right) + \left[\frac{\Delta z}{\sigma\Delta t}\left(\theta_{s,i} - \theta_{r,i}\right) - \left(\left(\frac{\partial q_-^n}{\partial S_i^n}\right) - \left(\frac{\partial q_+^n}{\partial S_i^n}\right)\right)\right]\left(S_i^{n+1} - S_i^n\right)$$
$$+\left(\frac{\partial q_+^n}{\partial S_{i+1}^n}\right)\left(S_{i+1}^{n+1} - S_{i+1}^n\right) = q_-^n - q_+^n \tag{8}$$

The Newton-Raphson method was initially developed as a root-finding algorithm of an arbitrary equation that has been generalized for solving a system of non-linear equations. Applied to the soil moisture form of the RE and using an implicit scheme, the NR consists in defining a residual based on the mass balance equation (Eq. (6)) at iteration k for time step $n+1$ and for cell i written as:

$$R_i^{n+1,k} = \frac{\Delta z}{\Delta t}\left(\theta_{s,i} - \theta_{r,i}\right)\left(S_i^{n+1,k} - S_i^n\right) + q_+^{n+1,k} - q_-^{n+1,k} \tag{9}$$

where $R_i^{n+1,k}$ is called the residual.

The NR consists in computing the solution at iteration $k+1$ by estimating the residual of the next iteration $R_i^{n+1,k+1}$ using a first order Taylor development and setting it equal to zero as:

$$\frac{R_i^{n+1,k}}{\partial S^{n+1,k}}\left(S_i^{n+1,k+1} - S_i^{n+1,k}\right) + R_i^{n+1,k} = 0 \tag{10}$$

The derivatives of this residual are:

$$\begin{cases} \dfrac{\partial R_i^{n+1,k}}{\partial S_{i-1}^{n+1,k}} = -\dfrac{\partial q_-^{n+1,k}}{\partial S_{i-1}^{n+1,k}} \\[3mm] \dfrac{\partial R_i^{n+1,k}}{\partial S_i^{n+1,k}} = \dfrac{\Delta z}{\Delta t}\left(\theta_{s,i} - \theta_{r,i}\right) + \dfrac{\partial q_+^{n+1,k}}{\partial S_i^{n+1,k}} - \dfrac{\partial q_-^{n+1,k}}{\partial S_i^{n+1,k}} \\[3mm] \dfrac{\partial R_i^{n+1,k}}{\partial S_{i+1}^{n+1,k}} = \dfrac{\partial q_+^{n+1,k}}{\partial S_{i+1}^{n+1,k}} \end{cases} \tag{11}$$

which leads to the following set of linear equations:

$$-\frac{\partial q_-^{n+1,k}}{\partial S_{i-1}^{n+1,k}}\left(S_{i-1}^{n+1,k+1} - S_{i-1}^{n+1,k}\right) + \left[\frac{\Delta z}{\Delta t}\left(\theta_{s,i} - \theta_{r,i}\right) + \frac{\partial q_+^{n+1,k}}{\partial S_i^{n+1,k}} - \frac{\partial q_-^{n+1,k}}{\partial S_i^{n+1,k}}\right]\left(S_i^{n+1,k+1} - S_i^{n+1,k}\right)$$

$$+\frac{\partial q_+^{n+1,k}}{\partial S_{i+1}^{n+1,k}}\left(S_{i+1}^{n+1,k+1} - S_{i+1}^{n+1,k}\right) = \frac{\Delta z}{\Delta t}\left(\theta_{s,i} - \theta_{r,i}\right)\left(S_i^{n+1,k} - S_i^n\right) + q_+^{n+1,k} - q_-^{n+1,k} \tag{12}$$

For the first iteration, we have $S_i^{n+1,k+1} = S_i^{n+1}$ and $S_i^{n+1,k} = S_i^n$, and therefore :

$$-\frac{\partial q_-^n}{\partial S_{i-1}^n}\left(S_{i-1}^{n+1}-S_{i-1}^n\right)+\left[\frac{\Delta z}{\Delta t}\left(\theta_{s,i}-\theta_{r,i}\right)+\frac{\partial q_+^n}{\partial S_i^n}-\frac{\partial q_-^n}{\partial S_i^n}\right]\left(S_i^{n+1}-S_i^n\right)$$

$$+\frac{\partial q_+^n}{\partial S_{i+1}^n}\left(S_{i+1}^{n+1}-S_{i+1}^n\right)=q_+^n-q_-^n \tag{13}$$

Whatever the formulation of the fluxes q (as a function of the pressure (see eq. A1) or the water content, expressed by Kirchhoff transform as in Ross (2003) or not), the implicit Ross method (eq. (8) with $\sigma=1$)) is equivalent to the first iteration of the Newton-Raphson method (eq. (13)).

3. Newton Raphson method for the mixed form Richards' equation

Because the pressure-based formulation does not ensure mass conservation - except for the approximation provided by Rathfelder and Abriola (1994) - and due to the limitations of the moisture-based formulation (see previous section), the mixed formulation has been widely used since the work of Celia et al. (1990).

The mixed form of the Richards equation given by equation (1) is rewritten as:

$$\frac{\partial\theta}{\partial t}+S_w s_0\frac{\partial\psi}{\partial t}=\nabla\cdot k_r(\psi)\mathbf{K}\left[\nabla\psi+\nabla z\right]+f \tag{14}$$

and is discretized by:

$$\mathbf{A}^{n+1,k}\boldsymbol{\psi}^{n+1,k+1}+\mathbf{B}^{n+1,k}\frac{\boldsymbol{\psi}^{n+1,k+1}-\boldsymbol{\psi}^n}{\Delta t^{n+1}}+\mathbf{E}\frac{\boldsymbol{\theta}^{n+1,k+1}-\boldsymbol{\theta}^n}{\Delta t^{n+1}}=\mathbf{F}^{n+1,k} \tag{15}$$

where $\mathbf{A}$ is the discretized form of the divergence term, $\mathbf{B}$ and $\mathbf{E}$ are the discretized forms of the storage terms and $\mathbf{F}$ is the discretized form of the sink/source term and the boundary conditions, n is the time step and k the iteration counter. Δt^{n+1} is the time step magnitude defined by $\Delta t^{n+1}=t^{n+1}-t^n$. Matrices $\mathbf{A, B, E}$ and vector $\mathbf{F}$ depend on the numerical scheme used for the spatial discretization. The implicit scheme is applied for the spatial discretization.

For the Newton-Raphson method, the residual is defined now by:

$$\mathbf{R}(\psi^{n+1,k}) = \mathbf{A}^{n+1,k}\psi^{n+1,k} + \mathbf{B}^{n+1,k}\frac{\psi^{n+1,k}-\psi^{n}}{\Delta t^{n+1}} + \mathbf{E}\frac{\theta^{n+1,k}-\theta^{n}}{\Delta t^{n+1}} - \mathbf{F}^{n+1,k} \qquad (16)$$

and its derivatives are:

$$\mathbf{R}'(\psi^{n+1,k}) = \mathbf{A}^{n+1,k} + \frac{\partial \mathbf{A}^{n+1,k}}{\partial \psi^{n+1,k}}\psi^{n+1,k} + \frac{\mathbf{B}^{n+1,k}}{\Delta t^{n+1}} + \frac{\partial \mathbf{B}^{n+1,k}}{\partial \psi^{n+1,k}}\frac{\psi^{n+1,k}-\psi^{n}}{\Delta t^{n+1}}$$
$$+ \frac{\mathbf{E}}{\Delta t^{n+1}}\frac{\partial \theta^{n+1,k}}{\partial \psi^{n+1,k}} - \frac{\partial \mathbf{F}^{n+1,k}}{\partial \psi^{n+1,k}} \qquad (17)$$

Looking for $\psi^{n+1,k+1}$ such as $\mathbf{R}(\psi^{n+1,k+1}) = 0$, the system to solve is similar to Eq. (10):

$$\mathbf{R}'(\psi^{n+1,k})\Delta\psi^{n+1,k+1} = -\mathbf{R}(\psi^{n+1,k}) \qquad (18)$$

with $\Delta\psi^{n+1,k+1} = \psi^{n+1,k+1} - \psi^{n+1,k}$.

The NR formulation is also used for the non-iterative scheme by applying only one NR step per time step, with $\psi^{n+1} = \psi^{n+1,1}$ where $\psi^{n+1,0} = \psi^{n}$ (Paniconi et al., 1991; Zha et al., 2015).

4. Algorithms and time stepping strategy

The usual algorithm used to solve RE consists in defining a time step that remains constant and to iteratively compute the parameters and variables in the following way:

For a given time step n

Define the time step length Δt^{n+1} depending on the time stepping strategy.

Initialization of the iterative process by setting $\psi^{n+1,1} = \psi^{n}$.

do k=1, maxit

1. Computation of the variable $\theta^{n+1,k}$, the parameter $\mathbf{K}^{n+1,k}$ and their derivatives $\dfrac{d\theta^{n+1,k}}{d\psi^{n+1,k}}, \dfrac{\partial \mathbf{K}^{n+1,k}}{\partial \psi^{n+1,k}}$ using $\psi^{n+1,k}$.

2. Computation of the system matrix $\mathbf{R}'$ and the residual $\mathbf{R}$.

3. Computation of the system solution $\psi^{n+1,k+1}$.

4. Check convergence. If convergence is achieved, exit.

10

enddo

Next time step

where *k* is the iteration counter and *maxit* the maximum number of iterations.

The time-adaptive algorithm consists in calculating the non-linear parameters with the pressure heads computed at time step n and adapting the time step length. The algorithm is described by the following:

For a given time step n

Computation of the variable $\mathbf{\theta}^n$, the parameter $\mathbf{K}^n$ and their derivatives $\dfrac{d\mathbf{\theta}^n}{d\mathbf{\psi}^n}, \dfrac{\partial \mathbf{K}^n}{\partial \mathbf{\psi}^n}$ using $\mathbf{\psi}^n$.

do k=1, maxit

1. Define a time step $\Delta t^{n+1,k}$ depending on the time stepping strategy.
2. Computation of the system matrix $\mathbf{R}'$ and the residual $\mathbf{R}$.
3. Computation of the system solution $\mathbf{\psi}^{n+1,k+1}$.
4. Check convergence. If convergence is achieved, exit.

enddo

Next time step

The main advantage of the alternative algorithm is its avoidance of the computation of the variable $\mathbf{\theta}$, the parameter $\mathbf{K}$ and their derivatives $\dfrac{d\mathbf{\theta}}{d\mathbf{\psi}}$ and $\dfrac{\partial \mathbf{K}}{\partial \mathbf{\psi}}$ during the iterations. Due to the highly nonlinear relations between $\mathbf{\theta}$, $\mathbf{K}$, $\dfrac{d\mathbf{\theta}}{d\mathbf{\psi}}$, $\dfrac{\partial \mathbf{K}}{\partial \mathbf{\psi}}$ and the pressure, this computation may require significant CPU time.

The most popular time step management during the simulation is that of the heuristic type (Miller et al., 2006). The time step Δt^{n+1} is computed depending on Δt^n and the number of iterations *k* necessary to reach convergence in the following way:

$$\begin{cases} if \quad k \leq m_1 & \Delta t^{n+1} = k_1 \Delta t^n & k_1 > 1.0 \\ if \quad m_1 \leq k \leq m_2 & \Delta t^{n+1} = \Delta t^n & \\ if \quad m_2 \leq k & \Delta t^{n+1} = k_2 \Delta t^n & k_2 < 1.0 \end{cases} \quad (19)$$

11

where k_1, k_2, m_1, m_2 are user-defined constants.

Other heuristic time step management procedures have been suggested by Kirkland et al., (1992) based on the water volumes exchanged between the adjacent cells of the grid and by Ross (2003), where the time step size is controlled by the maximum allowed change in the saturation.

For the Ross method, the fluxes are computed first and the time step magnitude is calculated accordingly using

$$\Delta t^{n+1} = \frac{\Delta S_{max}}{\max_i \left(\frac{\left| q_{-,i}^n - q_{+,i}^n \right|}{\Delta z_i \left(\theta_{s,i} - \theta_{r,i} \right)} \right)} \tag{20}$$

where ΔS_{max} is the user-defined maximum allowed saturation change. After the computation of the change in the saturation ΔS, the time step is modified if the maximum of the computed change exceeds $(1+\lambda) max_i \left(|\Delta S_i| \right)$, where λ is a user-defined value, according to:

$$\Delta t^{n+1,k} = \frac{\Delta S_{max}}{\max_i \left(|\Delta S_i| \right)} \Delta t^{n+1,k-1} \tag{21}$$

and the system of equations is solved again. More details about handling the fluxes at boundaries and saturated conditions can be found in Crevoisier et al. (2009), Ross (2003) and Varado et al. (2006b).

The adaptive scheme used in this work evaluates the time steps through truncation error due to the temporal discretization as proposed by Thomas and Gladwell (1988). This scheme was already applied to the pressure-based formulation by Kavetski et al. (2001) and to the moisture-based formulation by Kavetski and Binning (2004).

The difference between the first-order and second-order time approximations can be considered as an estimate of the local truncation error of the first-order scheme. The first-order approximation is given by:

$$\boldsymbol{\psi}_{(1)}^{n+1} = \boldsymbol{\psi}^n + \Delta t^{n+1} \frac{\partial \boldsymbol{\psi}^n}{\partial t} \tag{22}$$

The second-order approximation is:

12

$$\psi_{(2)}^{n+1} = \psi^n + \Delta t^{n+1} \frac{\partial \psi^n}{\partial t} + \frac{1}{2} \left(\Delta t^{n+1} \right)^2 \frac{\partial^2 \psi^n}{\partial t^2}$$

$$= \psi^n + \frac{1}{2} \left(\Delta t^{n+1} \right) \left[\frac{\partial \psi^{n+1}}{\partial t} + \frac{\partial \psi^n}{\partial t} \right]$$

(23)

using $\dfrac{\partial \psi^{n+1}}{\partial t} = \dfrac{\partial \psi^n}{\partial t} + \Delta t^{n+1} \dfrac{\partial^2 \psi^n}{\partial t^2}$.

This truncation error is given by:

$$\varepsilon_t^{n+1} = \max_i \left| \psi_{(2),i}^{n+1} - \psi_{(1),i}^{n+1} \right| = \frac{1}{2} \Delta t^{n+1} \max_i \left| \frac{\partial \psi_i^{n+1}}{\partial t} - \frac{\partial \psi_i^n}{\partial t} \right|$$

$$\approx \frac{1}{2} \Delta t^{n+1} \max_i \left| \frac{\psi_i^{n+1} - \psi_i^n}{\Delta t^{n+1}} - \frac{\psi_i^n - \psi_i^{n-1}}{\Delta t^n} \right|$$

(24)

When the truncation error is smaller than γ, the temporal truncation error tolerance defined by the user, the size of the next time step is calculated by:

$$\Delta t^{n+1} = \Delta t^n \min \left(s \sqrt{\frac{\gamma}{\max(\varepsilon_t^{n+1}, EPS)}}, r_{\max} \right)$$

(25)

When the truncation error is larger than γ, the computation is repeated with a reduced time step defined as following:

$$\Delta t^n = \Delta t^n \max \left(s \sqrt{\frac{\gamma}{\max(\varepsilon_t^{n+1}, EPS)}}, r_{\min} \right)$$

(26)

where r_{max} and r_{min} are user-defined constants used to avoid too drastic changes of the time step. s is considered to be a safety factor that ensures that the time step changes are reasonable. *EPS* is used to avoid floating point errors when the truncation error becomes too small.

5. Evaluation of the algorithms' performance

We applied the NR method to the mixed form of RE using the standard iterative algorithm and the time-adaptive algorithm. A cell centered finite volume scheme for the spatial discretization with an implicit Euler-scheme for the temporal discretization has been used to solve the partial differential equation and arithmetic means are used to compute the inter-block hydraulic conductivity. The detailed discretizations of the matrix $\mathbf{R}'(\boldsymbol{\psi}^{n+1,k})$ and the vector $\mathbf{R}(\boldsymbol{\psi}^{n+1,k})$ (see Eq.(18)) are given in Appendix 1. The time-adaptive algorithms have been applied as described by the authors: Ross (2003) for the time stepping based on the saturation changes and Kavetski et al. (2001) for the time stepping based on the truncation errors.

For the standard iterative algorithm, we defined two types of errors to check the convergence: the error based on the maximum change of the state variables between two iterations defined by $\varepsilon_\psi = \max_i \left| \psi_i^{n+1,k+1} - \psi_i^{n+1,k} \right|$ and the truncation error ε_t defined by Eq. (24). Convergence is assumed to be achieved when:

$$\varepsilon_\psi < \tau_{\psi,a} + \tau_{\psi,r} \left| \psi_{imax}^{n+1,k+1} \right| \tag{27}$$

where $\tau_{\psi,a}$ and $\tau_{\psi,r}$ are the absolute and relative user-defined tolerances and $\psi_{imax}^{n+1,k+1}$ is the pressure corresponding to ε_ψ and when:

$$\varepsilon_t < \tau_{t,a} + \tau_{t,r} \left| \psi_{imax}^{n+1,k+1} \right| \tag{28}$$

where $\tau_{t,a}$ and $\tau_{t,r}$ have the same meaning as those for the previous criterion but $\psi_{imax}^{n+1,k+1}$ represents the pressure value corresponding to ε_t.

The tested algorithms are summarized in Table 1. Computations of all possible combinations for the standard iterative scheme have been performed. We present only the four most

14

efficient algorithms. We also analyzed convergence based on the non-linear residual. It was found less restrictive than the previous criteria. Due to the definition of the NR method, the residual tends to zero but it does not ensure a small value of ε_ψ. Therefore, the results related to the reduction of the non-linear residuals are not reported.

We investigated three one-dimensional problems with various initial and boundary conditions and hydraulic functions to assess the accuracy, efficiency and computational costs of the different algorithms. The selected test cases represent a range of difficult infiltration problems widely analyzed in the literature:

- TC1: infiltration in a homogeneous initially dry soil with constant prescribed pressure at the surface and prescribed pressure at the bottom (Celia et al., 1990);

- TC2: infiltration in a homogeneous soil initially at hydrostatic equilibrium with a prescribed constant flux at the soil surface and prescribed pressure at the bottom (Miller et al., 1998);

- TC3: infiltration/evaporation in an initially dry heterogeneous soil, with variable positive and negative fluxes at the surface and free drainage at the base of the soil column (Lehmann and Ackerer, 1998).

For the three test cases, the soil hydraulic functions were described by Mualem-Van Genuchten models (Mualem, 1976; van Genuchten, 1980), see Eq. (4) and (5).

The required parameters, boundary conditions and initial conditions are summarized in Table 2. The evolution of the relative hydraulic conductivity, the water saturation and the specific moisture capacity with respect to the pressure values are shown in Figures 1, 2 and 3, respectively. For TC1, the pressure will vary from -1000 cm to -75 cm only due to the specific conditions of this test case. Therefore, the parameter variations are smaller than those

for the other test cases. Since the parameters' variations are more abrupt for test cases 2 and 3, their solutions are more challenging.

Preliminary tests were performed to define the optimal spatial discretization i.e. a finer spatial discretization provided very similar results for a given convergence criterion and a given time stepping strategy. Therefore, we can assume that the errors are only originated from the time step size and the linearization.

The following criteria were used for the time stepping strategy:

- k_1=0.80, k_2=1.20, m_1=5, m_2=10, which are the usual values for the heuristic strategy defined by Eq. (19);
- r_{min}=0.10, r_{max}=4.0, s=0.9, EPS=10^{-10}, which are the standard values for the time stepping scheme based on time discretization error defined by Eq. (26) (Kavetski et al., 2001).

To perform a consistent comparison of the time step strategies, the maximum allowed change in saturation (see equation (20) and (21)) has been evaluated using the maximum change in the pressure, according to the following relationship:

$$\Delta S_{max} \approx \frac{1}{\left(\theta_{s,imax} - \theta_{r,imax}\right)} \frac{d\theta}{d\psi}\bigg|_{imax}^{n} \left(\tau_a + \tau_r \left|\psi_{imax}^{n+1,k+1}\right|\right) \tag{29}$$

The simulations have been performed using different values of τ_r and with $\tau_a = 0.0$.

We used several criteria to evaluate the performance of these codes. A typical error used in solving RE is the global cumulative mass balance error defined by:

$$MB(t^{n+1}) = \frac{\sum_{i=1}^{M} \Delta z_i \left(\theta_i^{n+1} - \theta_i^0\right)}{\sum_{k=1}^{n+1} \left(q_{in}^k - q_{out}^k\right)\Delta t^k} \tag{30}$$

16

where Δz_i is the size of the cell/element i, θ_i^{n+1} is its water content at time t^{n+1}, θ_i^0 is the initial water content, and q_{in}^k and q_{out}^k are the inflow and outflow, respectively, at the domain boundaries at time t^k. M is the number of cells/elements. The fluxes at the boundaries are defined by $q^k = \frac{1}{2}\left(q^k + q^{k-1}\right)$. The mass balance errors were checked for each runs but were found to be negligible since we solved the mass-conserving RE form.

While it is necessary to satisfy the global mass balance for an accurate numerical scheme, a low mass balance error is not sufficient to ensure the accuracy of the solution. Therefore, solutions have also been compared with the reference solution obtained using a very fine temporal discretization and the iterative Newton-Raphson method. This comparison is based on the average relative error defined by:

$$\varepsilon_k = \left[\frac{1}{M} \sum_i \frac{\left| \psi_i^{ref} - \hat{\psi}_i \right|^k}{\left| \psi_i^{ref} \right|^k} \right]^{1/k} \tag{31}$$

where M is the number of cells, $\mathbf{\psi}^{ref}$ is the reference solution and $\hat{\mathbf{\psi}}$ is the tested numerical solution. ε_1 represents the average absolute relative error (called L_1-norm in the following), ε_2 is the average quadratic error (L_2-norm) and ε_∞ is the highest local relative difference between the numerical and the reference solutions (L_∞-norm).

Since the time-adaptive algorithm does not require the computation of the parameters and their derivatives during the iterative procedure, we use N_{sol} to denote the number of times where the system of equations is solved and N_{param} to denote the number of times where the parameters are computed. Of course, these counters are equal to each other for the standard algorithm, which leads to computational costs depending on $2N_{sol}$. N_{param} is less than N_{sol} for the time-adaptive algorithm. For comparison purposes, the computational costs are estimated

by N_{sol} for the standard algorithm and by $(N_{sol} + N_{param})/2$ for the time-adaptive algorithm. The efficiency of the algorithms have been evaluated by comparing the computational costs for a given relative tolerance τ_r. The errors are presented in the tables and the figures. The figures show some additional results not listed in the tables that already contains much information.

TC1: Infiltration in a homogenous soil with constant boundary conditions

This test case simulates an infiltration into a homogeneous porous medium. This problem is addressed here because it has been widely analyzed previously by many authors like Bouchemella et al. (2015), Celia et al. (1990), El Kadi and Ling (1993), Rathfelder and Abriola, (1994), Tocci et al. (1997), among others. The computations were performed with a spatial discretization of 0.1 cm. The initial time step size was set to $1.0 \ 10^{-5}$ s, and the maximum time step size was set to 400 s.

The results for the iterative and time-adaptive algorithms are presented in Tables 3 and 4, respectively. When both convergence criteria are used (algorithms SH_$\Delta\psi$_Δt and SS_$\Delta\psi$_Δt), N_{trunc} represents the number of times where the truncation error is the most restrictive condition. For the heuristic time stepping schemes, the convergence is mostly linked to the truncation error (N_{trunc} is close to N_{sol}), whereas when the saturation time stepping scheme is used, the most restrictive criterion is the maximum difference in the pressure.

When the time stepping scheme is based on saturation, for both iterative and time-adaptive algorithms, the number of iterations required to solve the problem is proportional to the relative tolerance. Therefore, highly accurate solutions incur high computational costs.

For the time-adaptive scheme, the number of parameter changes N_{param} is close to the number of iterations for low tolerance values. Small tolerance values lead to small time steps,

avoiding time step adjustments. This is not the case for larger tolerance values that lead to larger time steps and therefore to additional iterations (see for example TA_T for the tolerance of $\tau_r = 10^{-2}$ – Table 4).

The three types of errors provide the same information. The best solution for one type of error is also the best solution for the two others.

On average, the iterative algorithm is faster than the time-adaptive algorithm that requires more iterations for a given error. This is also shown in Figure 4 that presents the convergence rate of the L_2-norm with respect to the computational costs, *i.e.,* the number of iterations or number of iterations and number of parameter changes. The time-adaptive algorithm with time stepping based on the truncation errors performs quite poorly compared to the other algorithms. Irrespective of the tolerance, this algorithm leads to a wetting front moving faster (Fig. 5).

When the relative tolerance is set to a very low value ($\tau_r = 10^{-5}$), the iterative scheme with time stepping based on the saturation changes shows behavior that is different from that found for the less restrictive tolerance. The criterion based on truncation errors is no longer significant ($N_{trunc}=252$), possibly explaining why the accuracy of the scheme remains constant. This also indicates that errors due to time discretization have to be handled, either in the convergence criterion or in the time stepping strategy.

For this test case, the most efficient algorithms are the iterative algorithms using the time stepping strategy based on truncation error (ST_$\Delta\psi$) or based on the saturation changes (SS_$\Delta\psi$_Δt). Saturated based time stepping strategies (SS_$\Delta\psi$_Δt and TA_S) shows a linear decrease of L_2 with computational costs. For very high precision ($L_2 < 10^{-4}$), ST_$\Delta\psi$ outperforms the other algorithms. No convincing explanation has been found for the insignificant change in accuracy for SS_$\Delta\psi$_Δt at high precision.

19

TC2: Infiltration in a homogenous soil with hydrostatic initial conditions

This test case models an infiltration in a 200 cm vertical column of unconsolidated clay loam with non-uniform grain size distribution and was considered by Miller et al. (1998) to be a very challenging test. This problem was found to be more challenging from the numerical point of view compared to TC1 due to the relative permeability function that enhances the non-linear behavior of Richards' equation (Fig. 1, 2, 3). The cell size has been set to 0.125 cm, the initial time step to 10^{-5}s and the maximum time step magnitude to 1000 s.

The different norms for the iterative and the time-adaptive schemes are given in Tables 5 and 6.

Investigation of this test case leads to similar qualitative conclusions when the time stepping scheme is based on the saturation differences (SS_$\Delta\psi$_Δt and TA_S). The standard scheme SH_$\Delta\psi$ fails to provide an accurate solution within a reasonable number of iterations (less than 10^7).

The most efficient methods are the schemes using the time stepping strategy based on truncation errors (Fig. 6). However, as found for TC1, the adaptive time algorithm TA_T failed to provide highly accurate results (L_2-norm error less than approximately 4.5 10^{-4}).

Figure 7 shows the time step magnitudes for approximately equal L_2-norms for the two time-adaptive algorithms and for the iterative algorithm using truncation errors for time stepping (4.254 10^{-4} within 3503 iterations for ST_$\Delta\psi$, 4.563 10^{-4} within 3098 iterations for TA_T and 4.844 10^{-4} within 11358 iterations for TA_S). The time step evolution is very similar for the three strategies: a linear increase until around 0.1s, followed by a very slow increase until 20-30s and a regular increase until the end of the simulation. ST_$\Delta\psi$ and TA_T strategies lead to

the same time steps when time reaches 1s. The time step sizes remain smaller for TA_S which explains the significant higher number of iterations required to solve this test case.

TC3: Infiltration/evaporation in a heterogeneous soil

This case study simulates infiltration in an initially dry heterogeneous soil with a succession of rainfall and evaporations as upper boundary conditions during 35 days. This problem differs from the two previous cases by the soil heterogeneity and also by the non-monotonic boundary conditions at the soil surface. It is expected that non-monotonic discontinuous boundary conditions will increase the difficulty of finding accurate solutions. The soil profile consists of three 60 cm thick layers. The layers are discretized using cells with the size of 0.10 cm. The prescribed fluxes are changing every day. For a given time, these fluxes are linearly interpolated. To avoid a too rough time discretization of these boundary conditions, the maximum time step magnitude has been fixed at 0.20 day. The initial time step is set to 10^{-5} day.

The relative errors estimated by the iterative algorithms and the time-adaptive algorithms are presented in Tables 7 and 8, respectively, and are plotted in Figure 8.

The standard iterative scheme fails to converge within the maximum number of iterations (10^7) when the tolerance is not sufficiently restrictive. The detailed analyses of the computation showed that the time step size was quite large compared to the more restrictive conditions until day 28.0 where the infiltration fluxes were equal to 1.50 cm/day and where the conditions were near saturation due to the previous infiltration period. This led to a decrease of the time step to close to the minimum value (10^{-8} s), causing the procedure to stop. More restrictive conditions lead to smaller time steps from the beginning of the simulation and a better approximation of the solutions during the entire simulation.

21

The iterative scheme coupled with the truncation based time step strategy showed a surprisingly unstable behavior for $\tau_r = 10^{-3}$. The scheme did not converge for $\tau_r \in \left[0.96\,10^{-3}; 1.04\,10^{-3} \right]$. The results presented in Table 7 and Figure 8 are obtained for $\tau_r = 0.90\,10^{-3}$. At this stage of our work, we were not able to provide a meaningful explanation for this effect.

The time-adaptive algorithm with the saturation based time stepping scheme is the most efficient for an L_2-norm greater than 10^{-4}. For more accurate results, the iterative method with the time stepping strategy using the truncation error must be preferred. The impact of the time stepping strategy for these two algorithms is shown in Figure 9 for approximately the same L_2-norm ($2.051\,10^{-3}$ within 1283 iterations for TA_S and $1.517\,10^{-3}$ within 6504 iterations for ST_$\Delta\psi$). The time step changes is related to the boundary conditions variations as expected. The strategy based on the saturation variation leads to a longer time step than the strategy using the time truncation error. This difference can be quite important (see the simulation between days 25 and 30). The consequences of this difference are a reduced number of iterations but also a less accurate computation, irrespective of the error norm.

6. Summary and conclusions

The solution of RE is complex and very time consuming due to its highly non-linear properties. Several algorithms have been tested for the mixed-form of Richards equation, including time-adaptive methods. Based on the numerical examples that differ in their parameters (level of non-linearity) and in their initial and boundary conditions, the conclusions and recommendations are:

1. Our numerical developments showed that the method suggested by Ross (2003) in its implicit formulation can be considered as a Newton-Raphson method with a time-adaptive algorithm.

2. The different algorithms have different convergence rates (accuracy improvement of the scheme as a function of the computational costs). Therefore, an algorithm can be very efficient for a given accuracy and less efficient for another level of precision. However, for these three test cases and in average, the best performance in terms of efficiency was obtained using a stopping criterion based on truncation error with its corresponding time step strategy (ST_$\Delta\psi$). Similar results were obtained by Kavetski et al. (2001) for the pressure-based RE and by Kavetski and Binning (2004) for the moisture-based RE.

3. The mass balance is not a good criterion for the evaluation of the results because the mixed-form preserves the mass balance, irrespective of the pressure distribution within the profile.

4. The time truncation error should be implemented in numerical codes using the standard iterative procedure. The use of the maximum variable difference between two successive iterations only, which is usually implemented, does not provide any information about the accuracy of the time derivative approximation.

Our 1-dimensional examples showed that time-adaptive algorithm TA_T is very sensitive to the type of problem to solve. The time-adaptive algorithm TA_S was less efficient than the usual schemes. However, for a larger amount of elements like in 2D or 3D problems, this conclusion might be different because the time dedicated to the computation of the parameters can be significant higher, unless tabulated values are used to evaluate the parameters and the required derivatives.

Depending on the type of the problem that must be solved (parameters behavior with respect to the pressure, time variations of the boundary conditions), the time truncation errors may be predominant compared to the error corresponding to the pressure changes between two successive iterations. Therefore, we recommend the implementation of this stopping criteria associated with the time stepping strategy as defined by Kavetski et al. (2001).

References

Bause, M., Knabner, P., 2004. Computation of variably saturated subsurface flow by adaptive mixed hybrid finite element methods. Adv. Water Resour. 27, 565–581. doi:10.1016/j.advwatres.2004.03.005

Belfort, B., Younes, A., Fahs, M., Lehmann, F., 2013. On equivalent hydraulic conductivity for oscillation–free solutions of Richard's equation. J. Hydrol. 505, 202–217. doi:10.1016/j.jhydrol.2013.09.047

Bergamaschi, L., Putti, M., 1999. Mixed finite elements and Newton-type linearizations for the solution of Richards' equation. Int. J. Numer. Methods Eng. 45, 1025–1046. doi:10.1002/(SICI)1097-0207(19990720)45

Bouchemella, S., Seridi, A., Alimi-Ichola, I., 2015. Numerical simulation of water flow in unsaturated soils: comparative study of different forms of Richards's equation. Eur. J. Environ. Civ. Eng. 19, 1–26. doi:10.1080/19648189.2014.926294

Celia, M.A., Bouloutas, E.T., Zarba, R.L., 1990. A general mass-conservative numerical solution for the unsaturated flow equation. Water Resour. Res. 26, 1483–1496. doi:10.1029/WR026i007p01483

Clark, M. P., Fan Y., Lawrence D. M., Adam J. C., Bolster D., Gochis D. J., Hooper R. P., Kumar M., Leung L. R., Mackay D. S., Maxwell R. M., Shen C., Swenson S. C., Zeng, X., 2015. Improving the representation of hydrologic processes in Earth System Models. Water Resour. Res., 51, 5929–5956, doi:10.1002/2015WR017096.

Crevoisier, D., Chanzy, A., Voltz, M., 2009. Evaluation of the Ross fast solution of Richards' equation in unfavourable conditions for standard finite element methods. Adv. Water Resour. 32, 936–947. doi:10.1016/j.advwatres.2009.03.008

Diersch, H.-J.G., Perrochet, P., 1999. On the primary variable switching technique for simulating unsaturated–saturated flows. Adv. Water Resour. 23, 271–301. doi:10.1016/S0309-1708(98)00057-8

El Kadi, A.I., Ling, G., 1993. The Courant and Peclet Number criteria for the numerical solution of the Richards Equation. Water Resour. Res. 29. doi:10.1029/93WR00929

Fahs, M., Younes, A., Lehmann, F., 2009. An easy and efficient combination of the Mixed Finite Element Method and the Method of Lines for the resolution of Richards' Equation. Environ. Model. Softw. 24, 1122–1126. doi:10.1016/j.envsoft.2009.02.010

Farthing, M.W., Kees, C.E., Miller, C.T., 2003. Mixed finite element methods and higher order temporal approximations for variably saturated groundwater flow. Adv. Water Resour. 26, 373–394. doi:10.1016/S0309-1708(02)00187-2

Feddes, R.A., Kabat, P., Van Bakel, P.J.T., Bronswijk, J.J.B., Halbertsma, J., 1988. Modelling soil water dynamics in the unsaturated zone — State of the art. J. Hydrol. 100, 69–111. doi:10.1016/0022-1694(88)90182-5

Forsyth, P.A., Wu, Y.S., Pruess, K., 1995. Robust numerical methods for saturated-unsaturated flow with dry initial conditions in heterogeneous media. Adv. Water Resour. 18, 25–38. doi:10.1016/0309-1708(95)00020-J

Gottardi, G., Venutelli, M., 2001. UPF: two-dimensional finite-element groundwater flow model for saturated–unsaturated soils. Comput. Geosci. 27, 179–189. doi:10.1016/S0098-3004(00)00082-0

Hirthe, E.M., Graf, T., 2012. Non-iterative adaptive time-stepping scheme with temporal truncation error control for simulating variable-density flow. Adv. Water Resour. 49, 46–55. doi:10.1016/j.advwatres.2012.07.021

Kavetski, D., Binning, P., 2004. Truncation error and stability analysis of iterative and non-iterative Thomas–Gladwell methods for first-order non-linear differential equations. Int. J. Numer. Methods Eng. 60, 2031–2043. doi:10.1002/nme.1035

Kavetski, D., Binning, P., 2002a. Adaptive backward Euler time stepping with truncation error control for numerical modelling of unsaturated fluid flow. Int. J. Numer. Methods Eng. 53, 1301–1322. doi:10.1002/nme.329

Kavetski, D., Binning, P., 2002b. Noniterative time stepping schemes with adaptive truncation error control for the solution of Richards equation. Water Resour. Res. 38. doi:10.1029/2001WR000720

Kavetski, D., Binning, P., Sloan, S.W., 2001. Adaptive time stepping and error control in a mass conservative numerical solution of the mixed form of Richards equation. Adv. Water Resour. 24, 595–605. doi:10.1016/S0309-1708(00)00076-2

Kirkland, M.R., Hills, R.G., Wierenga, P.J., 1992. Algorithms for solving Richards' equation for variably saturated soils. Water Resour. Res. 28, 2049–2058.

Lehmann, F., Ackerer, P., 1998. Comparison of Iterative Methods for Improved Solutions of the Fluid Flow Equation in Partially Saturated Porous Media. Transp. Porous Media 31, 275–292. doi:10.1023/A:1006555107450

Matthews, C.J., Braddock, R.D., Sander, G.C., 2004. Modeling flow through a one-dimensional multi-layered soil profile using the Method of Lines. Environ. Model. Assess. 9, 103–113.

Miller, C.T., Abhishek, C., Farthing, M.W., 2006. A spatially and temporally adaptive solution of Richards' equation. Adv. Water Resour. 29, 525–545. doi:10.1016/j.advwatres.2005.06.008

Miller, C.T., Williams, G.A., Kelley, C.T., Tocci, M.D., 1998. Robust solution of Richards' equation for nonuniform porous media. Water Resour. Res. 34, 2599–2610. doi:10.1029/98WR01673

Mualem, Y., 1976. A new model for predicting the hydraulic conductivity of unsaturated porous media. Water Resour. Res. 12, 513–522. doi:10.1029/WR012i003p00513

Paniconi, C., Aldama, A.A., Wood, E.F., 1991. Numerical evaluation of iterative and noniterative methods for the solution of the nonlinear Richards equation. Water Resour. Res. 27, 1147–1163.

Paniconi, C., Putti, M., 1994. A comparison of Picard and Newton iteration in the numerical solution of multidimensional variably saturated flow problems. Water Resour. Res. 30, 3357–3374. doi:10.1029/94WR02046

R. G. Hills, I.P., 1989. Modeling one-dimensional infiltration into very dry soils: 1. Model development and evaluation. Water Resour. Res. 25. doi:10.1029/WR025i006p01259

Rathfelder, K., Abriola, L.M., 1994. Mass conservative numerical solutions of the head-based Richards equation. Water Resour. Res. 30, 2579–2586. doi:10.1029/94WR01302

Richards, L.A., 1931. Capillary conduction of liquids through porous medium. J. Appl. Phys. 1, 318–333. doi:10.1063/1.1745010

Romano, N., Brunone, B., Santini, A., 1998. Numerical analysis of one-dimensional unsaturated flow in layered soils. Adv. Water Resour. 21, 315–324. doi:10.1016/S0309-1708(96)00059-0

Ross, P.J., 2003. Modeling Soil Water and Solute Transport—Fast, Simplified Numerical Solutions. Agron. J. 95, 1352. doi:10.2134/agronj2003.1352

Ross, P.J., Bristow, K.L., 1990. Simulating Water Movement in Layered and Gradational Soils Using the Kirchhoff Transform. Soil Sci. Soc. Am. J. 54, 1519. doi:10.2136/sssaj1990.03615995005400060002x

Thomas, R.M., Gladwell, I., 1988. Variable-order variable-step algorithms for second-order systems. Part 1: The methods. Int. J. Numer. Methods Eng. 26, 39–53.

Tocci, M.D., Kelley, C.T., Miller, C.T., 1997. Accurate and economical solution of the pressure-head form of Richards' equation by the method of lines. Adv. Water Resour. 20, 1–14. doi:10.1016/S0309-1708(96)00008-5

van Dam, J.C., Feddes, R.A., 2000. Numerical simulation of infiltration, evaporation and shallow groundwater levels with the Richards equation. J. Hydrol. 233, 72–85. doi:10.1016/S0022-1694(00)00227-4

van Genuchten, M.T., 1980. A Closed-form Equation for Predicting the Hydraulic Conductivity of Unsaturated Soils1. Soil Sci. Soc. Am. J. 44, 892. doi:10.2136/sssaj1980.03615995004400050002x

Varado, N., Braud, I., Ross, P.J., 2006a. Development and assessment of an efficient vadose zone module solving the 1D Richards' equation and including root extraction by plants. J. Hydrol. 323, 258–275. doi:10.1016/j.jhydrol.2005.09.015

Varado, N., Braud, I., Ross, P.J., Haverkamp, R., 2006b. Assessment of an efficient numerical solution of the 1D Richards' equation on bare soil. J. Hydrol. 323, 244–257. doi:10.1016/j.jhydrol.2005.07.052

Vergnes, J. P., Decharme, B., Alkama, R., Martin, E., Habets, F., Douville, H., 2012. A simple groundwater scheme for hydrological and climate applications: Description and offline evaluation over France. Journal of Hydrometeorology, 13(4), 1149-1171.

Williams, G.A., Miller, C.T., Kelley, C.T., 2000. Transformation approaches for simulating flow in variably saturated porous media. Water Resour. Res. 36, 923–934. doi:10.1029/1999WR900349

Zha, Y., Shi, L., Ye, M., Yang, J., 2013. A generalized Ross method for two- and three-dimensional variably saturated flow. Adv. Water Resour. 54, 67–77. doi:10.1016/j.advwatres.2013.01.002

Zha, Y., Tso, M.C.-H., Shi, L., Yang, J., 2015. Comparison of Non iterative Algorithms Based on Different Forms of Richards' Equation. Environ. Model. Assess. 21, 357–370. doi:10.1007/s10666-015-9467-1

APPENDIX 1.

The numerical method used in the paper is implicit standard finite difference. For a cell i of the grid, the unsaturated flow equation (4) can be discretized in the following way:

$$
\begin{cases}
\dfrac{\theta_i^{n+1} - \theta_i^n}{\Delta t} + S_w s_0 \dfrac{\psi_i^{n+1} - \psi_i^n}{\Delta t} + \dfrac{q_{i+}^{n+1} - q_{i-}^{n+1}}{\Delta z_i} = f_i \\[3mm]
q_{i-}^{n+1} = -K_{i-}\left(\dfrac{\psi_i^{n+1} - \psi_{i-1}^{n+1}}{\Delta z_{i-}} - 1 \right) \\[3mm]
q_{i+}^{n+1} = -K_{i+}\left(\dfrac{\psi_{i+1}^{n+1} - \psi_i^{n+1}}{\Delta z_{i+}} - 1 \right)
\end{cases}
\tag{A1}
$$

where n is the time step, K_{i-} is the inter-block conductivity between cell i and (i-1) defined by $K_{i-} = \dfrac{\Delta z_{i-1} K(\psi_{i-1}) + \Delta z_i K(\psi_i)}{\Delta z_{i-1} + \Delta z_i}$, K_{i+} is the inter-block conductivity between cell i and (i+1) defined by $K_{i+} = \dfrac{\Delta z_i K(\psi_i) + \Delta z_{i+1} K(\psi_{i+1})}{\Delta z_i + \Delta z_{i+1}}$. $\Delta z_{i-} = \dfrac{1}{2}\left(\Delta z_{i-1} + \Delta z_i \right)$ is the distance between the center of cell (i-1) and i. $\Delta z_{i+} = \dfrac{1}{2}\left(\Delta z_i + \Delta z_{i+1} \right)$ is the distance between the center of cell i and (i+1).

The residual is:

$$
R(\psi_i^{n+1,k}) = \Delta z_i \left(\theta_i^{n+1,k} - \theta_i^n \right) + \Delta z_i S_w s_0 \left(\psi_i^{n+1,k} - \psi_i^n \right) + \Delta t \left(q_{i+}^{n+1,k} - q_{i-}^{n+1,k} \right) - \Delta t \Delta z_i f_i
\tag{A2}
$$

where k is the iteration counter.

The residual derivatives are:

$$
\begin{aligned}
\frac{\partial R(\psi_i^{n+1,k})}{\partial \psi_{i-1}^{n+1,k}} &= -\Delta t \frac{\partial q_{i-}^{n+1,k}}{\partial \psi_{i-1}^{n+1,k}} \\[3mm]
\frac{\partial R(\psi_i^{n+1,k})}{\partial \psi_i^{n+1,k}} &= \Delta z_i \frac{d\theta_i^{n+1,k}}{d\psi_i^{n+1,k}} + \Delta z_i S_w s_0 + \Delta t \left(\frac{\partial q_{i+}^{n+1,k}}{\partial \psi_i^{n+1,k}} - \frac{\partial q_{i-}^{n+1,k}}{\partial \psi_i^{n+1,k}} \right) \\[3mm]
\frac{\partial R(\psi_i^{n+1,k})}{\partial \psi_{i+1}^{n+1,k}} &= \Delta t \frac{\partial q_{i+}^{n+1,k}}{\partial \psi_{i+1}^{n+1,k}}
\end{aligned}
\tag{A3}
$$

Therefore, the system to solve is:

$$-\Delta t \frac{\partial q_{i-}^{n+1,k}}{\partial \psi_{i-1}^{n+1,k}} \Delta \psi_{i-1}^{n+1,k+1} +$$

$$\left[\Delta z_i \frac{d\theta_i^{n+1,k}}{d\psi_i^{n+1,k}} + \Delta z_i S_w s_0 + \Delta t \left(\frac{\partial q_{i+}^{n+1,k}}{\partial \psi_i^{n+1,k}} - \frac{\partial q_{i-}^{n+1,k}}{\partial \psi_i^{n+1,k}} \right) \right] \Delta \psi_i^{n+1,k+1} +$$

$$\Delta t \frac{\partial q_{i+}^{n+1}}{\partial \psi_{i+1}^{n+1,k}} \Delta \psi_{i+1}^{n+1,k+1} =$$

$$-\Delta z_i \left(\theta_i^{n+1,k} - \theta_i^n \right) - \Delta z_i S_w s_0 \left(\psi_i^{n+1,k} - \psi_i^n \right) - \Delta t \left(q_{i+}^{n+1,k} - q_{i-}^{n+1,k} \right) + \Delta t \Delta z_i f_i$$

(A4)

With the following derivatives of the fluxes $q_{i-}^{n+1,k}$

$$\begin{cases} \dfrac{\partial q_{i-}^{n+1,k}}{\partial \psi_{i-1}^{n+1,k}} = -\dfrac{\partial K_{i-}^{n+1,k}}{\partial \psi_{i-1}^{n+1,k}} \left(\dfrac{\psi_i^{n+1,k} - \psi_{i-1}^{n+1,k}}{\Delta z_{i-}} - 1 \right) + \dfrac{K_{i-}^{n+1,k}}{\Delta z_{i-}} \\[4mm] \dfrac{\partial q_{i-}^{n+1,k}}{\partial \psi_i^{n+1,k}} = -\dfrac{\partial K_{i-}^{n+1,k}}{\partial \psi_i^{n+1,k}} \left(\dfrac{\psi_i^{n+1,k} - \psi_{i-1}^{n+1,k}}{\Delta z_{i-}} - 1 \right) - \dfrac{K_{i-}^{n+1,k}}{\Delta z_{i-}} \end{cases}$$

(A5)

and $q_{i+}^{n+1,k}$:

$$\begin{cases} \dfrac{\partial q_{i+}^{n+1,k}}{\partial \psi_i^{n+1,k}} = -\dfrac{\partial K_{i+}^{n+1,k}}{\partial \psi_i^{n+1,k}} \left(\dfrac{\psi_{i+1}^{n+1,k} - \psi_i^{n+1,k}}{\Delta z_{i+}} - 1 \right) + \dfrac{K_{i+}^{n+1,k}}{\Delta z_{i+}} \\[4mm] \dfrac{\partial q_{i+}^{n+1,k}}{\partial \psi_{i+1}^{n+1,k}} = -\dfrac{\partial K_{i+}^{n+1,k}}{\partial \psi_{i+1}^{n+1,k}} \left(\dfrac{\psi_{i+1}^{n+1,k} - \psi_i^{n+1,k}}{\Delta z_{i+}} - 1 \right) - \dfrac{K_{i+}^{n+1,k}}{\Delta z_{i+}} \end{cases}$$

(A6)

The component of the vector of the residuals $\mathbf{R}$ is given by equation (A2) and the coefficients of the matrix $\mathbf{R'}$ for cell i are:

$$R'_{i-1,i} = \Delta t \left[\frac{\partial K_{i-}^{n+1,k}}{\partial \psi_{i-1}^{n+1,k}} \left(\frac{\psi_i^{n+1,k} - \psi_{i-1}^{n+1,k}}{\Delta z_{i-}} - 1 \right) - \frac{K_{i-}^{n+1,k}}{\Delta z_{i-}} \right]$$

$$R'_{i,i} = \Delta z_i \left[\frac{d\theta_i^{n+1,k}}{d\psi_i^{n+1,k}} + S_w s_0 \right] - \Delta t \left[\frac{\partial K_{i+}^{n+1,k}}{\partial \psi_i^{n+1,k}} \left(\frac{\psi_{i+1}^{n+1,k} - \psi_i^{n+1,k}}{\Delta z_{i+}} - \right) - \frac{K_{i+}^{n+1,k}}{\Delta z_{i+}} \right]$$

(A7)

$$+ \Delta t \left[\frac{\partial K_{i-}^{n+1,k}}{\partial \psi_i^{n+1,k}} \left(\frac{\psi_i^{n+1,k} - \psi_{i-1}^{n+1,k}}{\Delta z_{i-}} - 1 \right) + \frac{K_{i-}^{n+1,k}}{\Delta z_{i-}} \right]$$

$$R'_{i,i+1} = -\Delta t \left[\frac{\partial K_{i+}^{n+1,k}}{\partial \psi_{i+1}^{n+1,k}} \left(\frac{\psi_{i+1}^{n+1,k} - \psi_i^{n+1,k}}{\Delta z_{i+}} - 1 \right) + \frac{K_{i+}^{n+1,k}}{\Delta z_{i+}} \right]$$

In case of prescribed flux at the upper boundary, the residual is written as:

$$R_1(\psi_1^{n+1,k}) = \Delta z_1 \left[\left(\theta_1^{n+1,k} - \theta_1^n \right) + S_w s_0 \left(\psi_1^{n+1,k} - \psi_1^n \right) \right] + \Delta t \left(q_{1+}^{n+1} - q_{BC} \right) - \Delta t \Delta z_1 f_1 \tag{A8}$$

Using the derivatives as defined in (A5) and (A6), the matrix coefficients are changed as follow:

$$R'_{1,1} = \Delta z_1 \left(\frac{d\theta_1^{n+1,k}}{d\psi_1^{n+1,k}} + S_w s_0 \right) - \Delta t \left[\frac{\partial K_{1+}^{n+1,k}}{\partial \psi_1^{n+1,k}} \left(\frac{\psi_2^{n+1,k} - \psi_1^{n+1,k}}{\Delta z_{1+}} - 1 \right) - \frac{K_{1+}^{n+1,k}}{\Delta z_{1+}} \right]$$

$$R'_{1,2} = -\Delta t \left[\frac{\partial K_{1+}^{n+1,k}}{\partial \psi_2^{n+1,k}} \left(\frac{\psi_2^{n+1,k} - \psi_1^{n+1,k}}{\Delta z_{1+}} - 1 \right) + \frac{K_{1+}^{n+1,k}}{\Delta z_{1+}} \right] \tag{A9}$$

If the flux is applied at the bottom of the profile, similar developments lead to the residual:

$$R_N = \Delta z_N \left[\left(\theta_N^{n+1,k} - \theta_N^n \right) + S_w s_0 \left(\psi_N^{n+1,k} - \psi_N^n \right) \right] + \Delta t \left(q_{BC} - q_{N-}^{n+1,k} \right) - \Delta t \Delta z_N f_N \tag{A10}$$

and its derivatives

$$R'_{N-1,N} = \Delta t \left[\frac{\partial K_{N-}^{n+1,k}}{\partial \psi_{N-1}^{n+1,k}} \left(\frac{\psi_N^{n+1,k} - \psi_{N-1}^{n+1,k}}{\Delta z_{N-}} - 1 \right) - \frac{K_{N-}^{n+1,k}}{\Delta z_{N-}} \right]$$

$$R'_{N,N} = \Delta z_N \left(\frac{d\theta_N^{n+1,k}}{d\psi_N^{n+1,k}} + S_w s_0 \right) + \Delta t \left[\frac{\partial K_{N-}^{n+1,k}}{\partial \psi_N^{n+1,k}} \left(\frac{\psi_N^{n+1,k} - \psi_{N-1}^{n+1,k}}{\Delta z_{N-}} - 1 \right) + \frac{K_{N-}^{n+1,k}}{\Delta z_{N-}} \right] \tag{A11}$$

If the pressure is described at the top of the soil, the corresponding flux is defined by:

$$q_{1-}^{n+1,k} = -K_{1-} \left(\frac{\psi_1^{n+1,k} - \psi_{BC}}{\Delta z_1 / 2} - 1 \right) \tag{A12}$$

And the derivative is:

$$\frac{\partial q_{1-}^{n+1,k}}{\partial \psi_1^{n+1,k}} = -\frac{\partial K_{1-}^{n+1,k}}{\partial \psi_1^{n+1,k}} \left(\frac{\psi_1^{n+1,k} - \psi_{BC}}{\Delta z_1 / 2} - 1 \right) - \frac{K_{1-}^{n+1,k}}{\Delta z_1 / 2} \tag{A13}$$

The corresponding residual and the matrix coefficients are:

$$R_1 = \Delta z_1 \left[\left(\theta_1^{n+1,k} - \theta_1^n \right) + S_w s_0 \left(\psi_1^{n+1,k} - \psi_1^n \right) \right] + \Delta t \left(q_{1+}^{n+1,k} - q_{1-}^{n+1,k} \right) - \Delta t \Delta z_1 f_1 \tag{A14}$$

and

$$R'_{1,1} = \Delta z_1 \left(\frac{d\theta_1^{n+1,k}}{d\psi_1^{n+1,k}} + S_w s_0 \right) - \Delta t \left[\frac{\partial K_{1+}^{n+1,k}}{\partial \psi_1^{n+1,k}} \left(\frac{\psi_2^{n+1,k} - \psi_1^{n+1,k}}{\Delta z_{1+}} - 1 \right) - \frac{K_{1+}^{n+1,k}}{\Delta z_{1+}} \right]$$

$$+ \Delta t \left[\frac{\partial K_{1-}^{n+1,k}}{\partial \psi_1^{n+1,k}} \left(\frac{\psi_1^{n+1,k} - \psi_{BC}}{\Delta z_1 / 2} - 1 \right) + \frac{K_{1-}^{n+1,k}}{\Delta z_1 / 2} \right] \tag{A15}$$

$$R'_{1,2} = -\Delta t \left[\frac{\partial K_{1+}^{n+1,k}}{\partial \psi_2^{n+1,k}} \left(\frac{\psi_2^{n+1,k} - \psi_1^{n+1,k}}{\Delta z_{1+}} - 1 \right) + \frac{K_{1+}^{n+1,k}}{\Delta z_{1+}} \right]$$

Similarly, if the pressure is prescribed at the soils column's bottom, we have:

$$R_N = \Delta z_N \left[\left(\theta_N^{n+1,k} - \theta_N^n \right) + S_w s_0 \left(\psi_N^{n+1,k} - \psi_N^n \right) \right] + \Delta t \left(q_{N+}^{n+1,k} - q_{N-}^{n+1,k} \right) - \Delta t \Delta z_N f_N \tag{A16}$$

and

$$R'_{N-1,N} = \Delta t \left[\frac{\partial K_{N-}^{n+1,k}}{\partial \psi_{N-1}^{n+1,k}} \left(\frac{\psi_N^{n+1,k} - \psi_{N-1}^{n+1,k}}{\Delta z_{N-}} - 1 \right) - \frac{K_{N-}^{n+1,k}}{\Delta z_{N-}} \right]$$

$$R'_{N,N} = \Delta z_N \left(\frac{d\theta_N^{n+1,k}}{d\psi_N^{n+1,k}} + S_w s_0 \right) - \Delta t \left[\frac{\partial K_{N+}^{n+1,k}}{\partial \psi_N^{n+1,k}} \left(\frac{\psi_{BC} - \psi_N^{n+1,k}}{\Delta z_N / 2} - 1 \right) - \Delta t \frac{K_{N+}^{n+1,k}}{\Delta z_N / 2} \right]$$

$$+ \Delta t \left[\frac{\partial K_{N-}^{n+1,k}}{\partial \psi_N^{n+1,k}} \left(\frac{\psi_N^{n+1,k} - \psi_{N-1}^{n+1,k}}{\Delta z_{N-}} - 1 \right) + \frac{K_{N-}^{n+1,k}}{\Delta z_{N-}} \right] \tag{A17}$$

The numerical code is written in FORTRAN 90 and is available upon request.

List of Tables

Table 1. Different options of the tested algorithms. Reference to the corresponding equation in parenthesis.

Table 2: Domain size (L), initial conditions (IC), boundary conditions at the soil surface (BC_u) and at the soil bottom (BC_l), saturated hydraulic conductivity (K_s), residual and saturated water contents (θ_r, θ_s) and shape parameters (α, n) for the different test cases. Length and time units are centimeters and seconds.

Table 3: Relative errors and number of iterations obtained for the iterative algorithm depending on different convergence criteria for TC1.

Table 4: Relative errors and number of iterations obtained for the time-adaptive algorithm depending on different convergence criteria for TC1.

Table 5: Relative errors and number of iterations obtained for the iterative algorithm depending on different convergence criteria for TC2 (n.c.: non convergence in less than 10^7 iterations).

Table 6: Relative errors and number of iterations obtained for the time-adaptive algorithm depending on different convergence criteria for TC2.

Table 7: Relative errors and number of iterations obtained for the iterative algorithm depending on different convergence criteria for TC3 (n.c.: non convergence in less than 10^7 iterations, * convergence failed for 10^{-3}, τ_r =0.90 10^{-3}).

Table 8: Relative errors and number of iterations obtained for the time-adaptive algorithm depending on different convergence criteria for TC3.

	Standard iterative algorithm					Time-adaptive algorithm	
	Time stepping			Stopping criterion			
	Heuristic (19)	Truncation (25) (26)	Saturation (20) (21)	Pressure (27)	Truncation (28)	Truncation (25) (26)	Saturation (20) (21)
SH_$\Delta\psi$	x			x			
SH_$\Delta\psi$_Δt	x			x	x		
ST_$\Delta\psi$		x		x			
SS_$\Delta\psi$_Δt			x	x	x		
TA_T						x	
TA_S							x

Table 1: Different options of the tested algorithms. Reference to the corresponding equation in parenthesis.

	L	IC	BC_u	BC_l	K_s	θ_r	θ_s	α	η
TC1	30	-1000.0	$\psi = -75$	$\psi = -1000$	$9.22\ 10^{-3}$	0.102	0.368	0.0335	2.0
TC2	200	z-200	$q=3.7\ 10^{-5}$	$\psi = 0$	$7.18\ 10^{-5}$	0.095	0.410	0.019	1.31
TC3	60	-100.0	$q(t)$	$q(t)=K_M(t)$	$6.26\ 10^{-3}$	0.0286	0.366	0.028	2.239
	60	-100.0			$1.51\ 10^{-4}$	0.106	0.469	0.0104	1.395
	60	-100.0			$6.26\ 10^{-3}$	0.0286	0.366	0.028	2.239

Table 2: Domain size (L), initial conditions (IC), boundary conditions at the soil surface (BC_u) and at the soil bottom (BC_l), saturated hydraulic conductivity (K_s), residual and saturated water contents (θ_r, θ_s) and shape parameters (α, η) for the different test cases. $K_M(t)$ is the hydraulic conductivity of the last grid cell.
Length and time units are centimeters and seconds respectively.

Tol.	Algorithm	L_1	L_2	L_∞	N_{trunc}	N_{sol}
10^{-5}	**SH_Δψ**	$1.918 \ 10^{-3}$	$8.829 \ 10^{-3}$	0.106		2177
	SH_Δψ_Δt	$8.391 \ 10^{-6}$	$6.459 \ 10^{-5}$	$8.782 \ 10^{-4}$	542371	615880
	ST_Δψ	$3.968 \ 10^{-4}$	$1.045 \ 10^{-3}$	$3.512 \ 10^{-3}$		6160
	SS_Δψ_Δt	$1.136 \ 10^{-5}$	$3.406 \ 10^{-5}$	$2.817 \ 10^{-4}$	252	3920446
10^{-4}	**SH_Δψ**	$2.557 \ 10^{-3}$	$1.375 \ 10^{-2}$	0.168		1701
	SH_Δψ_Δt	$7.818 \ 10^{-5}$	$2.259 \ 10^{-4}$	$1.593 \ 10^{-3}$	170438	194420
	ST_Δψ	$1.331 \ 10^{-3}$	$1.316 \ 10^{-3}$	$1.181 \ 10^{-2}$		1950
	SS_Δψ_Δt	$8.607 \ 10^{-6}$	$3.525 \ 10^{-5}$	$3.899 \ 10^{-4}$	154597	392041
10^{-3}	**SH_Δψ**	$3.956 \ 10^{-3}$	$1.166 \ 10^{-2}$	0.125		1312
	SH_Δψ_Δt	$2.320 \ 10^{-4}$	$7.553 \ 10^{-4}$	$7.883 \ 10^{-3}$	52723	60303
	ST_Δψ	$2.241 \ 10^{-3}$	$5.702 \ 10^{-3}$	$1.792 \ 10^{-2}$		620
	SS_Δψ_Δt	$6.567 \ 10^{-5}$	$1.585 \ 10^{-4}$	$1.453 \ 10^{-3}$	9895	39110
10^{-2}	**SH_Δψ**	$6.559 \ 10^{-3}$	$1.716 \ 10^{-2}$	0.119		1018
	SH_Δψ_Δt	$2.224 \ 10^{-3}$	$7.923 \ 10^{-3}$	$7.111 \ 10^{-2}$	15540	17888
	ST_Δψ	$9.954 \ 10^{-3}$	$2.630 \ 10^{-2}$	$8.727 \ 10^{-2}$		243
	SS_Δψ_Δt	$8.283 \ 10^{-4}$	$2.271 \ 10^{-3}$	$1.478 \ 10^{-2}$	862	3804

Table 3: Relative errors and number of iterations obtained for the iterative algorithm depending on different convergence criteria for TC1.

Tol.	Algorithm	L_1	L_2	L_∞	N_{param}	N_{sol}
10^{-5}	**TA_T**	$5.016\ 10^{-3}$	$2.376\ 10^{-2}$	0.269	32197	35938
	TA_S	$6.152\ 10^{-6}$	$2.429\ 10^{-5}$	$2.561\ 10^{-4}$	9316700	9322946
10^{-4}	**TA_T**	$5.598\ 10^{-3}$	$2.580\ 10^{-2}$	0.284	10169	11520
	TA_S	$2.839\ 10^{-5}$	$1.363\ 10^{-4}$	$1.654\ 10^{-3}$	931616	938144
10^{-3}	**TA_T**	$1.524\ 10^{-2}$	$7.085\ 10^{-2}$	0.822	3231	4032
	TA_S	$2.537\ 10^{-4}$	$1.271\ 10^{-3}$	$1.568\ 10^{-2}$	93114	100898
10^{-2}	**TA_T**	$6.241\ 10^{-2}$	0.274	2.459	1023	1402
	TA_S	$2.519\ 10^{-3}$	$1.224\ 10^{-2}$	0.142	9267	18292

Table 4: Relative errors and number of iterations obtained for the time-adaptive algorithm depending on different convergence criteria for TC1.

Tol.	Algorithm	L_1	L_2	L_∞	N_{trunc}	N_{sol}
10^{-5}	**SH_$\Delta\psi$**	$6.966\ 10^{-3}$	$1.818\ 10^{-2}$	$5.878\ 10^{-2}$		573
	SH_$\Delta\psi$_Δt	$3.697.\ 10^{-4}$	$9.766\ 10^{-4}$	$3.332\ 10^{-3}$	53769	59643
	ST_$\Delta\psi$	$1.578\ 10^{-4}$	$4.254\ 10^{-4}$	$2.451\ 10^{-3}$		3503
	SS_$\Delta\psi$_Δt	-	-	-	-	n. c.
10^{-4}	**SH_$\Delta\psi$**	$6.966\ 10^{-3}$	$1.818\ 10^{-2}$	$5.878\ 10^{-2}$		509
	SH_$\Delta\psi$_Δt	$6.968\ 10^{-4}$	$1.979\ 10^{-3}$	$5.726\ 10^{-3}$	16557	18428
	ST_$\Delta\psi$	$5.814\ 10^{-4}$	$1.492\ 10^{-3}$	$6.711\ 10^{-3}$		1033
	SS_$\Delta\psi$_Δt	$3.279\ 10^{-6}$	$1.239\ 10^{-5}$	$8.603\ 10^{-5}$	0	2474120
10^{-3}	**SH_$\Delta\psi$**	$6.966\ 10^{-3}$	$1.818\ 10^{-2}$	$5.878\ 10^{-2}$		410
	SH_$\Delta\psi$_Δt	$3.699\ 10^{-3}$	$9.761\ 10^{-3}$	$3.275\ 10^{-2}$	4830	5444
	ST_$\Delta\psi$	$1.553\ 10^{-3}$	$4.226\ 10^{-3}$	$2.457\ 10^{-2}$		317
	SS_$\Delta\psi$_Δt	$2.355\ 10^{-5}$	$6.230\ 10^{-5}$	$2.341\ 10^{-4}$	0	247426
10^{-2}	**SH_$\Delta\psi$**	$6.892\ 10^{-3}$	$1.800\ 10^{-2}$	$5.780\ 10^{-2}$		309
	SH_$\Delta\psi$_Δt	$9.135\ 10^{-3}$	$2.409\ 10^{-2}$	$7.925\ 10^{-2}$	376	580
	ST_$\Delta\psi$	$2.756\ 10^{-3}$	$1.134\ 10^{-2}$	$7.715\ 10^{-2}$		180
	SS_$\Delta\psi$_Δt	$2.973\ 10^{-4}$	$7.884\ 10^{-4}$	$3.252\ 10^{-3}$	0	24757

Table 5: Relative errors and number of iterations obtained for the iterative algorithm depending on different convergence criteria for TC2 (n.c.: non convergence in less than 10^7 iterations).

Tol.	Algorithm	L_1	L_2	L_∞	N_{param}	N_{sol}
10^{-5}	**TA_T**	$1.230\ 10^{-4}$	$4.563\ 10^{-4}$	$3.346\ 10^{-3}$	3089	3098
	TA_S	$8.741\ 10^{-6}$	$2.308\ 10^{-5}$	$7.905\ 10^{-5}$	1136193	1136199
10^{-4}	**TA_T**	$1.572\ 10^{-3}$	$4.497\ 10^{-3}$	$2.404\ 10^{-2}$	986	987
	TA_S	$2.701\ 10^{-5}$	$7.219\ 10^{-5}$	$3.095\ 10^{-4}$	113616	113616
10^{-3}	**TA_T**	$4.707\ 10^{-3}$	$1.346\ 10^{-2}$	$7.169\ 10^{-2}$	323	323
	TA_S	$1.754\ 10^{-4}$	$4.844\ 10^{-4}$	$2.391\ 10^{-3}$	11358	11358
10^{-2}	**TA_T**	$5.220\ 10^{-3}$	$1.683\ 10^{-2}$	0.101	135	135
	TA_S	$1.596\ 10^{-3}$	$4.444\ 10^{-3}$	$2.243\ 10^{-2}$	1132	1132

Table 6: Relative errors and number of iterations obtained for the time-adaptive algorithm depending on different convergence criteria for TC2.

Tol.	Algorithm	L_1	L_2	L_∞	N_{trunc}	N_{sol}
10^{-5}	**SH_Δψ**	$9.994\ 10^{-3}$	$1.119\ 10^{-2}$	$1.554\ 10^{-2}$		1644
	SH_Δψ_Δt	$6.612\ 10^{-4}$	$7.346\ 10^{-4}$	$1.116\ 10^{-3}$	171636	190588
	ST_Δψ	$6.830\ 10^{-4}$	$7.775\ 10^{-4}$	$1.648\ 10^{-3}$		16984
	SS_Δψ_Δt	$7.185\ 10^{-5}$	$7.935\ 10^{-5}$	$1.297\ 10^{-4}$	197481	1646346
10^{-4}	**SH_Δψ**	$6.664\ 10^{-3}$	$7.280\ 10^{-3}$	$1.033\ 10^{-2}$		1734
	SH_Δψ_Δt	$3.512\ 10^{-3}$	$3.898\ 10^{-3}$	$5.811\ 10^{-3}$	57312	63956
	ST_Δψ	$1.300\ 10^{-3}$	$1.517\ 10^{-3}$	$2.412\ 10^{-3}$		6504
	SS_Δψ_Δt	$5.380\ 10^{-5}$	$6.536\ 10^{-5}$	$1.010\ 10^{-4}$	41073	186351
10^{-3}	**SH_Δψ**	-	-	-		n.c.
	SH_Δψ_Δt	$2.625\ 10^{-3}$	$2.899\ 10^{-3}$	$4.971\ 10^{-3}$	22047	24779
	ST_Δψ	$4.730\ 10^{-3}$	$5.422\ 10^{-3}$	$1.036\ 10^{-2}$		1297*
	SS_Δψ_Δt	$7.569\ 10^{-4}$	$8.820\ 10^{-4}$	$1.402\ 10^{-3}$	16474	31276
10^{-2}	**SH_Δψ**	-	-	-		n.c.
	SH_Δψ_Δt	$5.493\ 10^{-3}$	$6.306\ 10^{-3}$	$1.171\ 10^{-3}$	7438	8812
	ST_Δψ	$6.621\ 10^{-3}$	$7.402\ 10^{-3}$	$1.042\ 10^{-2}$		810
	SS_Δψ_Δt	$7.511\ 10^{-3}$	$8.780\ 10^{-3}$	$1.378\ 10^{-2}$	5838	7535

Table 7: Relative errors and number of iterations obtained for the iterative algorithm depending on different convergence criteria for TC3 (n.c.: non convergence in less than 10^7 iterations, * convergence failed for 10^{-3}, $\tau_r = 0.90\ 10^{-3}$).

Tol.	Algorithm	L_1	L_2	L_∞	N_{param}	N_{sol}
10^{-5}	**TA_T**	$9.814\ 10^{-3}$	$9.949\ 10^{-3}$	$1.286\ 10^{-2}$	8369	8703
	TA_S	$7.980\ 10^{-5}$	$8.797\ 10^{-5}$	$1.472\ 10^{-4}$	1357075	1357160
10^{-4}	**TA_T**	$1.731\ 10^{-2}$	$1.760\ 10^{-2}$	$2.748\ 10^{-2}$	2653	2934
	TA_S	$1.067\ 10^{-4}$	$1.247\ 10^{-4}$	$1.997\ 10^{-4}$	135386	135498
10^{-3}	**TA_T**	$2.922\ 10^{-2}$	$3.105\ 10^{-2}$	$4.545\ 10^{-2}$	889	1153
	TA_S	$1.433\ 10^{-4}$	$1.788\ 10^{-4}$	$3.367\ 10^{-4}$	13314	13397
10^{-2}	**TA_T**	$1.996\ 10^{-2}$	$2.449\ 10^{-2}$	$5.536\ 10^{-2}$	347	515
	TA_S	$1.851\ 10^{-3}$	$2.051\ 10^{-3}$	$3.925\ 10^{-3}$	1232	1283

Table 8: Relative errors and number of iterations obtained for the time-adaptive algorithm depending on different convergence criteria for TC3.

List of Figures

Figure 1: Relative hydraulic conductivity as a function of the pressure for the three test cases (L1, L2 and L3 are the three layers for test case 3).
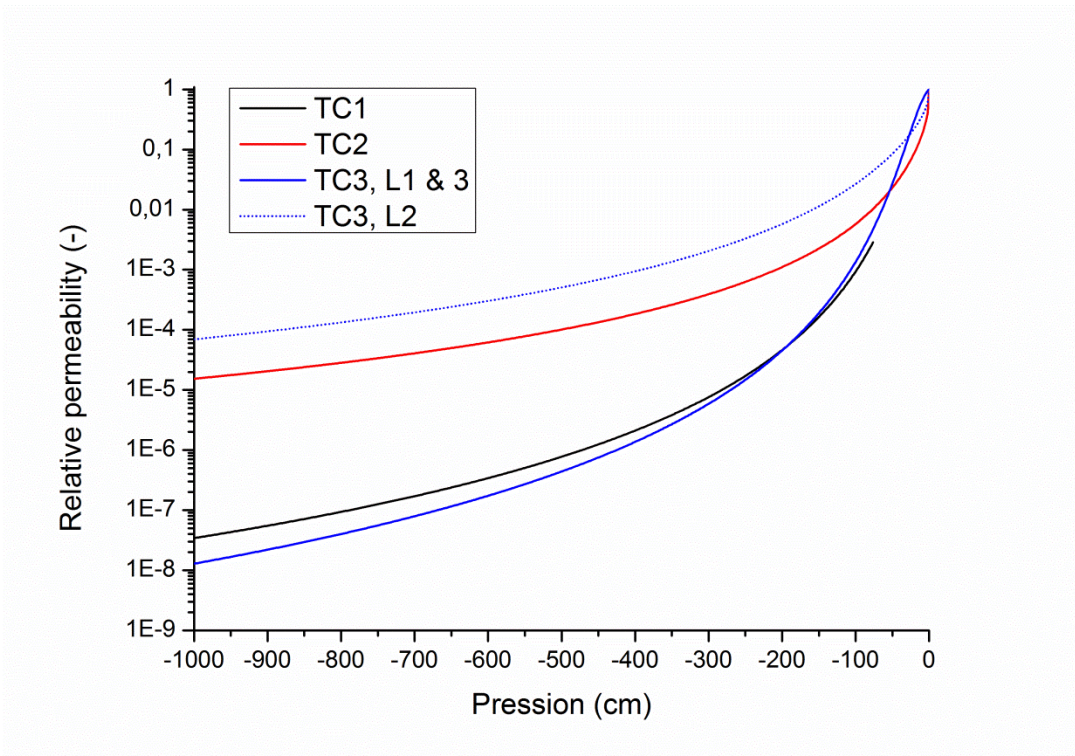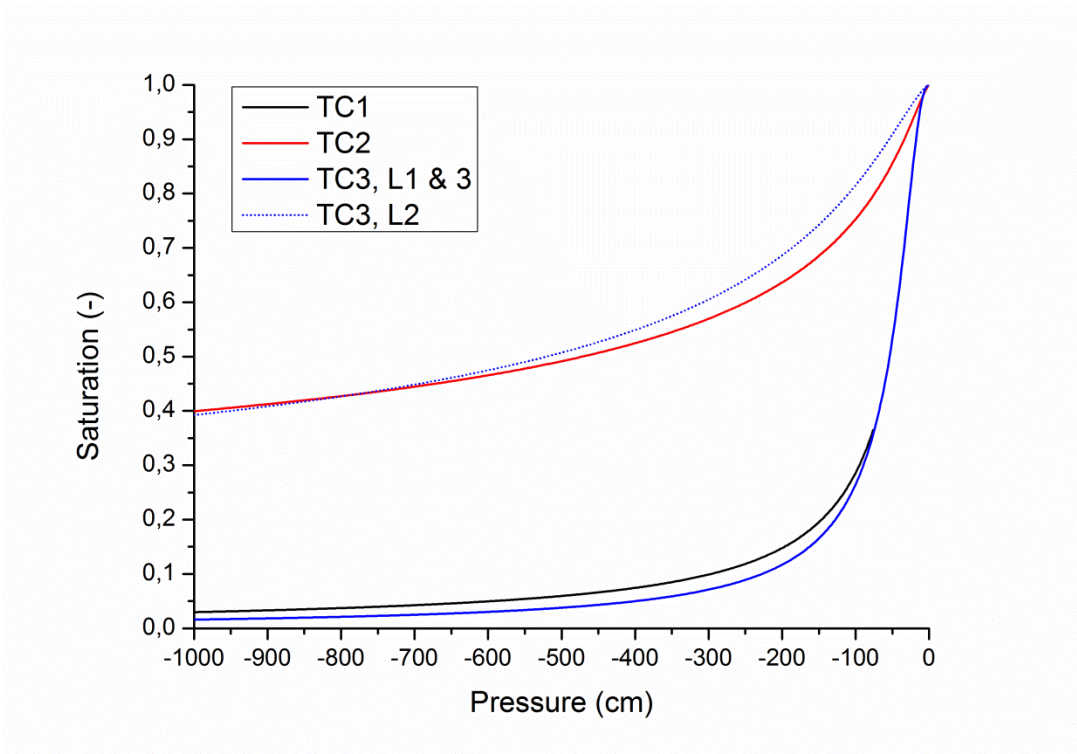
Figure 2: Water saturation as a function of the pressure for the three test cases (L1, L2 and L3 are the three layers for test case 3).
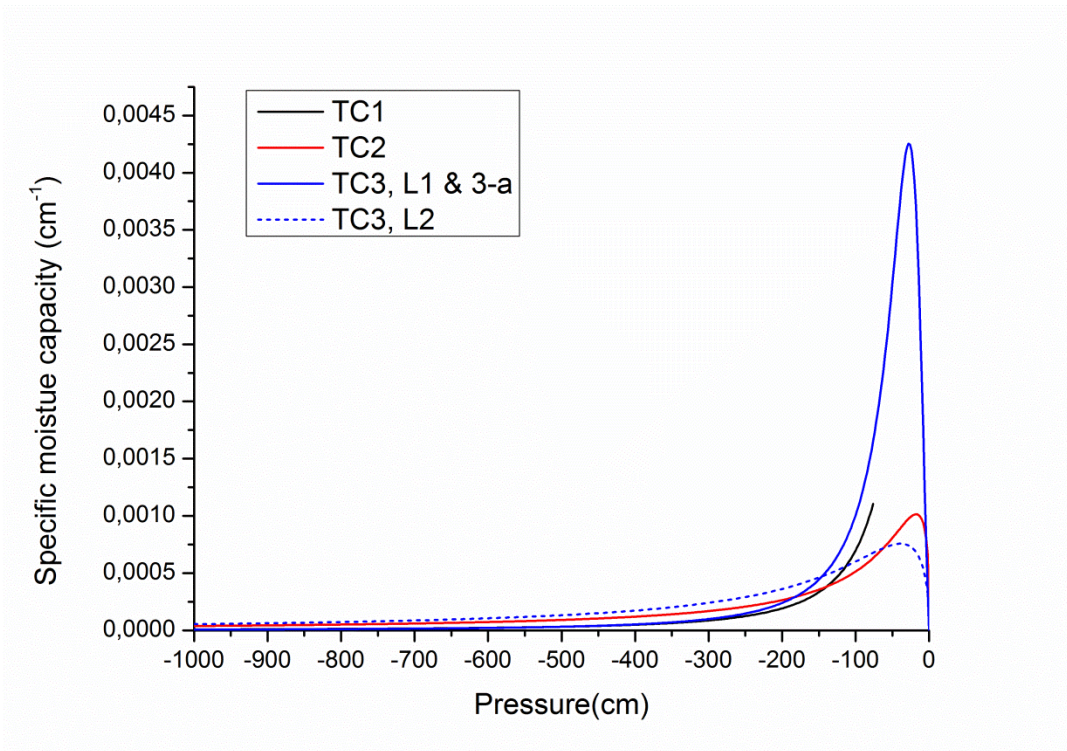
Figure 3: Specific moisture capacity as a function of the pressure for the three test cases (L1, L2 and L3 are the three layers for test case 3).
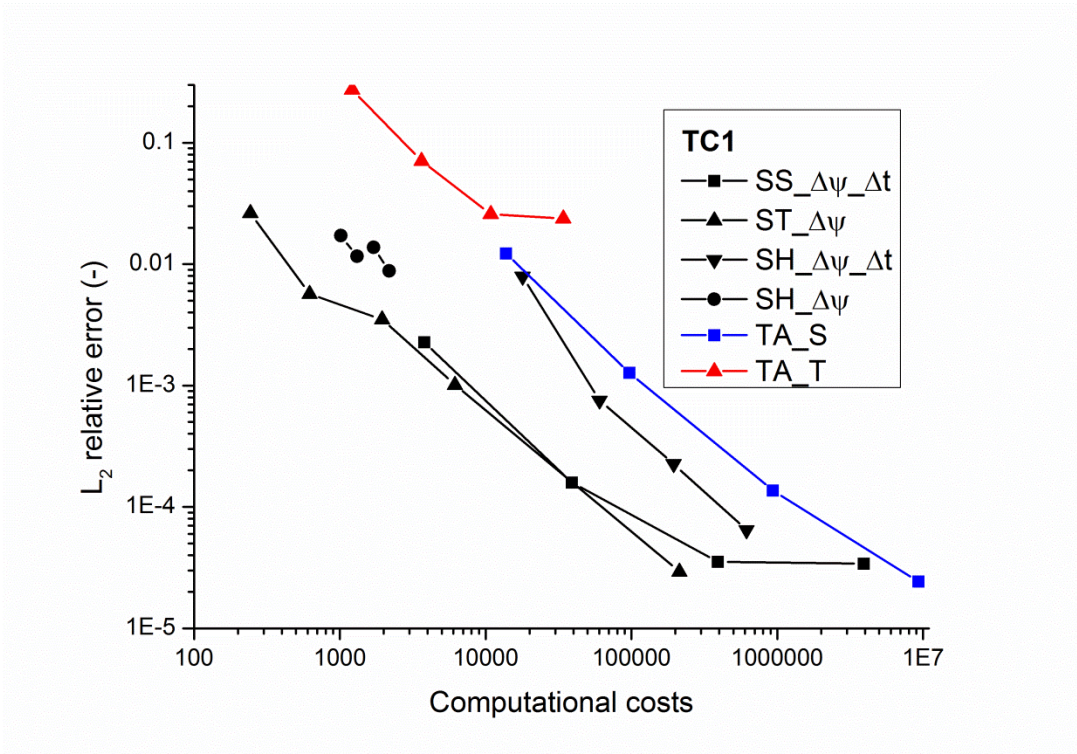
Figure 4: Evolution of the L_2 relative error with computational costs for TC1.
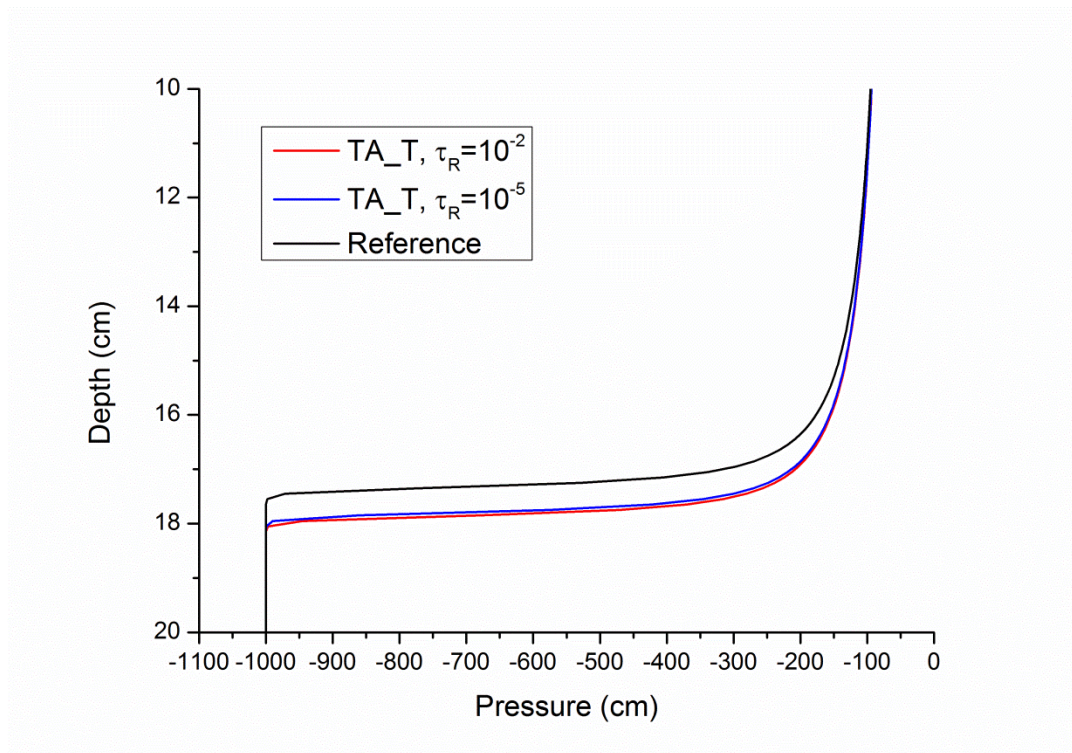
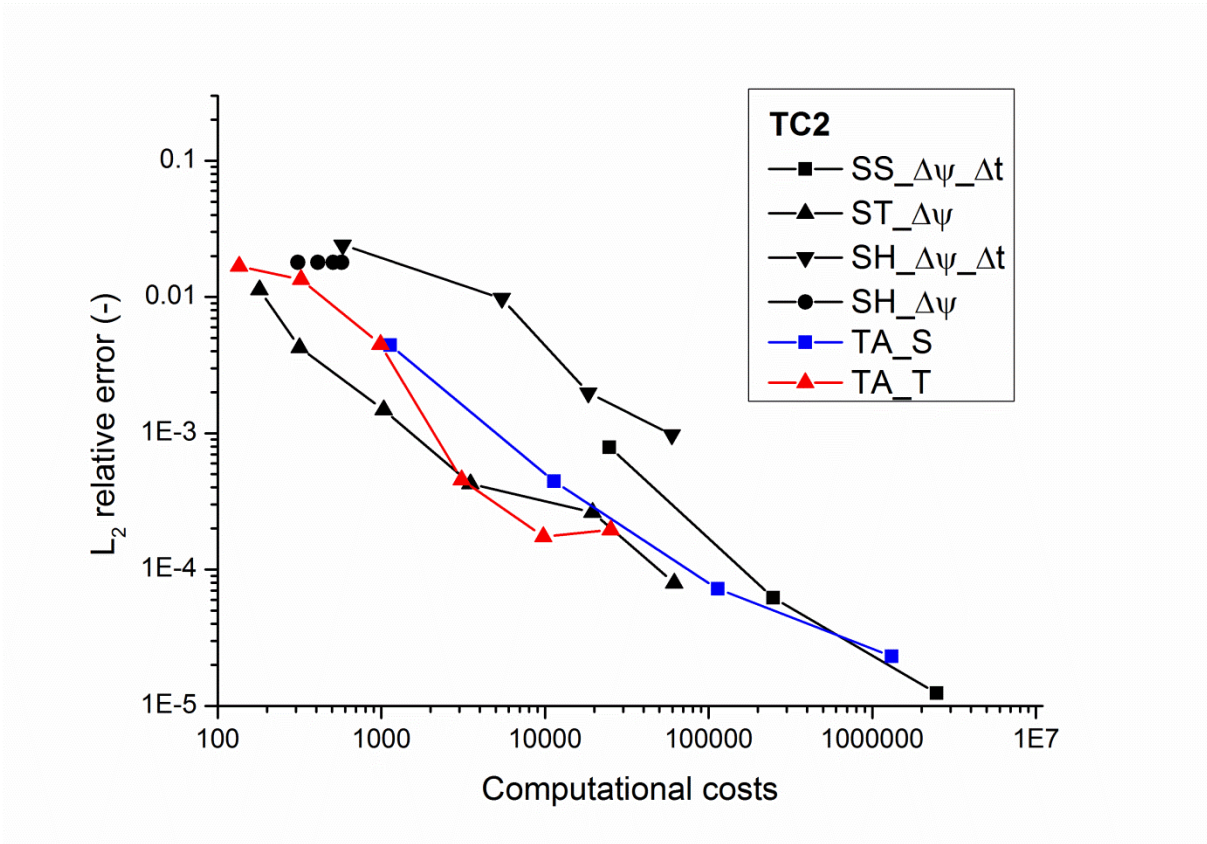Figure 5: Pressure profiles in the domain for the TA_T algorithm.

Figure 6: Evolution of the L_2 relative error with computational costs for TC2.
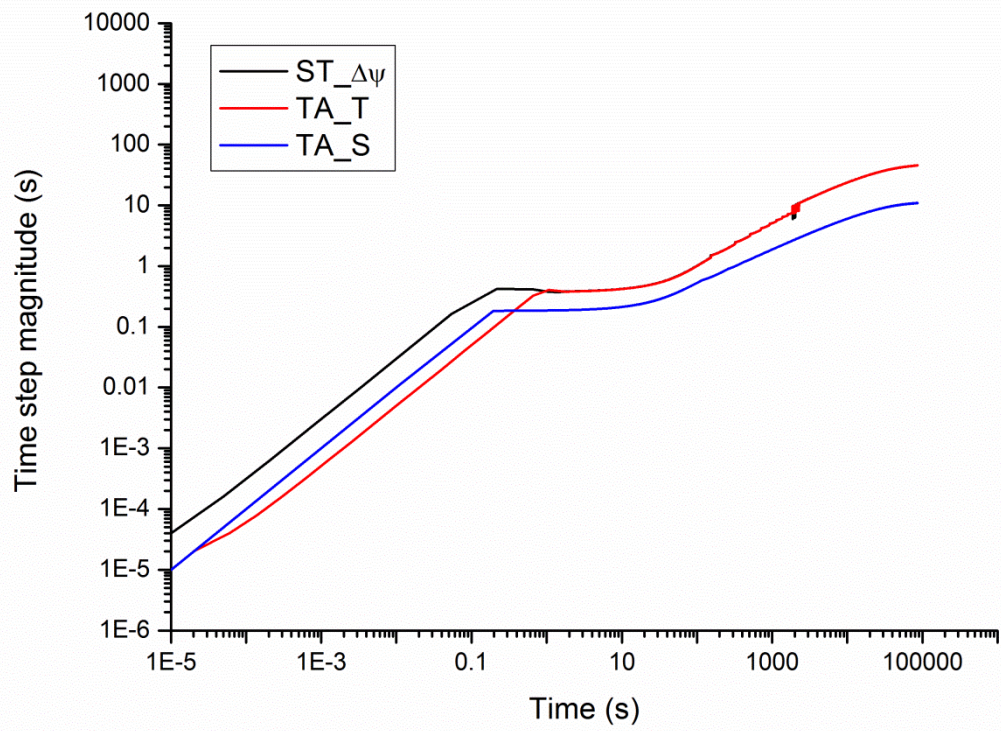
Figure 7: Time step magnitudes during the simulation for TC2.

Figure 8: Evolution of the L_2 relative error with computational costs for TC3.

Figure 9: Time step magnitudes during the simulation for TC3 for the time stepping strategy based on truncation error (TA_S in blue, TA_T in black, time varying boundary conditions at the top).

Figure 1: Relative permeability as a function of the pressure for the three test cases (L1, L2 and L3 are the three layers for test case 3).

Figure 2: Water saturation as a function of the pressure for the three test cases (L1, L2 and L3 are the three layers for test case 3).

Figure 3: Specific moisture capacity as a function of the pressure for the three test cases (L1, L2 and L3 are the three layers for test case 3).

Figure 4: Evolution of the L_2 relative error with computational costs for TC1.

Figure 5: Pressure profiles in the domain for the TA_T algorithm.

Figure 6: Evolution of the L_2 relative error with computational costs for TC2.

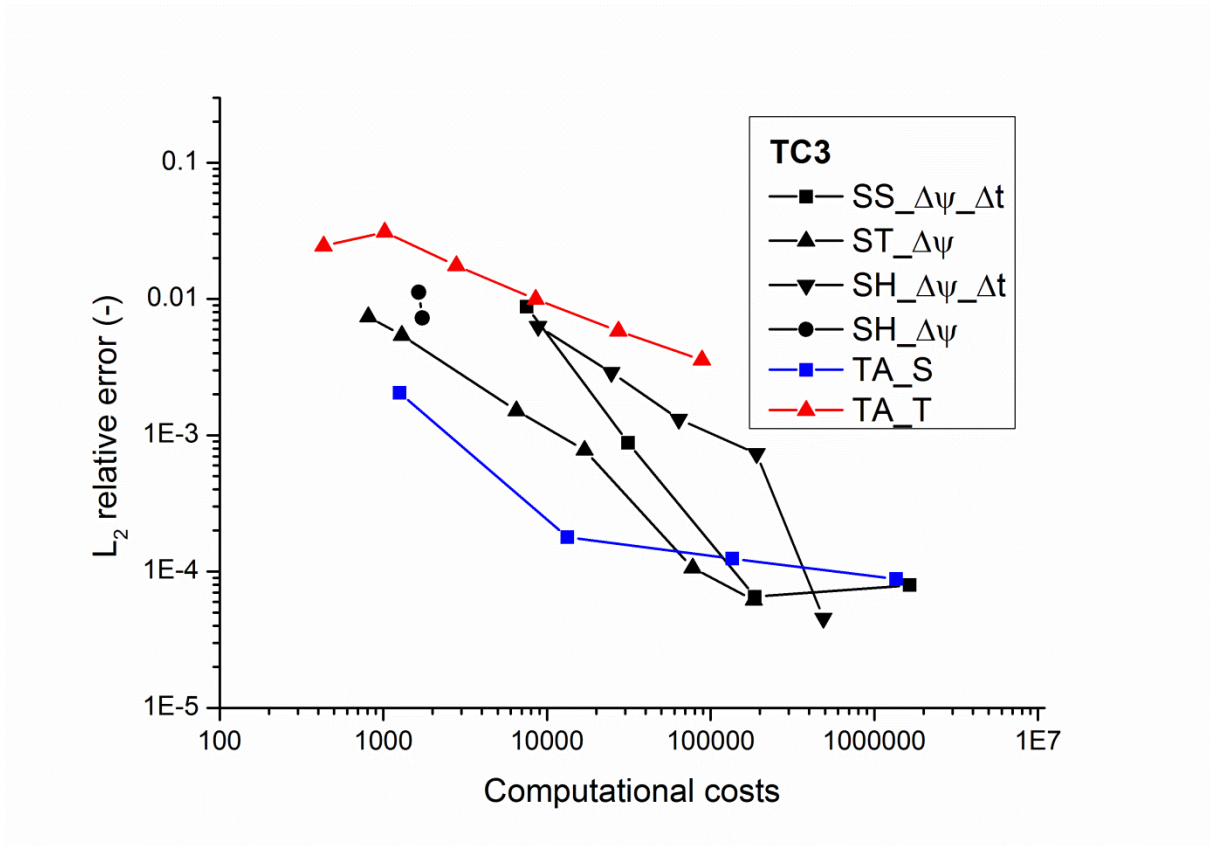Figure 7: Time step magnitudes during the simulation for TC2.

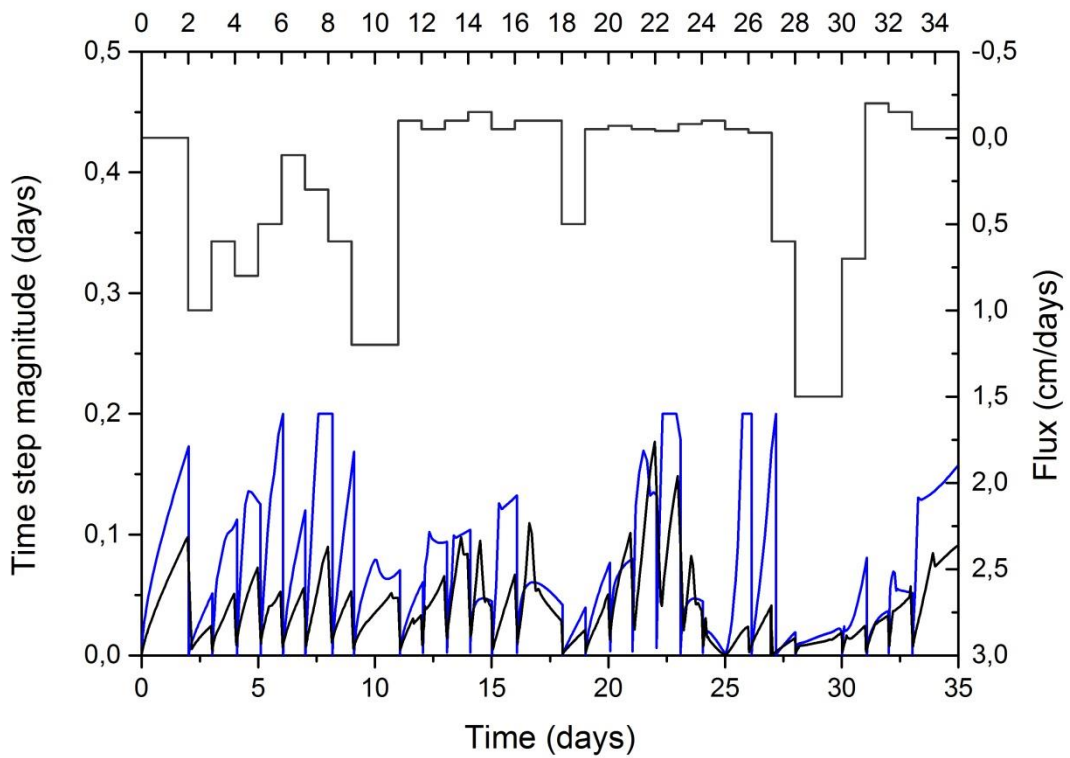Figure 8: Evolution of the L_2 relative error with computational costs for TC3.

Figure 9: Time step magnitudes during the simulation for TC3 for the time stepping strategy based on truncation error (TA_S in blue, TA_T in black, time varying boundary conditions at the top).